Spin transitions in non-classical systems

V. I. Ovcharenko,[a,b]★ K. Yu. Maryunina,[b] S. V. Fokin,[a] E. V. Tretyakov,[a] G. V. Romanenko,[a] and V. N. Ikorskii[a]

[a]*International Tomography Center, Siberian Branch of the Russian Academy of Science, 3a ul. Institutskaya, 630090 Novosibirsk, Russian Federation. Fax: +7 (383 2) 33 1399.*
[b]*Novosibirsk State University, 2 ul. Pirogova, 630090 Novosibirsk, Russian Federation. E-mail: Victor.Ovcharenko@tomo.nsc.ru*

Peculiarities of synthesis of chain polymeric, copper(II) hexafluoroacetylacetonate based complexes with stable nitroxyl radicals and the results of studies on correlations between the magnetic properties and structure of these compounds are summarized. Temperature variation causes structural rearrangements in the solid phases of the compounds, accompanied by the magnetic effects similar to spin crossover phenomena. Magnetic anomalies induced by phase transitions originate from specific motions in the Jahn—Teller coordination units containing two types of exchange clusters, $Cu^{2+}—O^{\bullet}—N<$ or $>N—^{\bullet}O—Cu^{2+}—O^{\bullet}—N<$, and are accompanied by significant changes in the crystal volume after multiple cooling/heating cycles. Chemical methods of controlling the character and temperature of spin transitions by both the formation of solid solutions of mixed-metal hexafluoroacetylacetonates with the same nitroxyl radical, $\{Cu_{1-x}M_x(hfac)_2L\}$ (M = Mn, Ni, Co), and by the formation of solid solutions based on copper(II) hexafluoroacetylacetonate with different nitroxyl radicals, $\{Cu(hfac)_2L_xL'_{1-x}\}$, are discussed. Specific influence of isotope substitution $CH_3 \rightarrow CD_3$ in the paramagnetic ligand on both the structure of the heterospin polymer chain and the temperature of the magnetic anomaly is discussed.

Key words: metal hexafluoroacetylacetonates, nitroxyl radicals, spin transitions, correlations between the magnetic properties and structure, solid solutions, isotope effect.

Introduction

The family of transition elements includes a group of d-elements (with d^4 to d^8 configurations) whose complexes can exhibit the so-called spin crossover effects consisting in transition of the central atom of a complex from a high-spin to a low-spin state on cooling, on increase in pressure, or on exposure to light.[1,2] Similarly to static loading, cooling leads to compression of a crystal, which in turn increases the splitting between the energy levels of the metal ion. If the difference between the crystal field induced splitting of terms and the energy of repulsion between electrons in low-lying d-orbitals is low, the compression of a crystal can cause an electronic transition from an upper-lying to a low-lying level, *i.e.*, a transition of the paramagnetic ion from the high-spin to the low-spin state. The effect is well known[3—12] and we will not dwell on this point. However, we emphasize that this kind of spin crossover is accompanied by a change in the ground-state spin multiplicity of one type of paramagnetic centers (here, the metal ions). From this point on these transitions will be called "spin transitions in classical systems" (STCS).

Recently, synthesized a number of polynuclear copper(II) complexes with stable nitroxyl radicals, which exhibit magnetic properties similar to those of the STCS, in particular, in character of the temperature dependence of the effective magnetic moment (μ_{eff}) were synthesized. Since the classical spin crossover in the copper(II) complexes with diamagnetic ligands (*i.e.*, in the systems containing only the d^9-paramagnetic centers) is impossible, the main difference between the spin transitions in the copper(II) complexes with nitroxyl radicals and the classical spin crossover is that the total spin of the heterospin exchange cluster containing two or more paramagnetic centers can change as a result of structural rearrangement in the coordination environment of the metal atom. For instance, the $Cu(hfac)_2$ tetranuclear complexes (hfac is hexafluoroacetylacetonate anion) with 3-pyridyl-substituted nitronylnitroxyl were reported.[13] Their magnetic behavior, similar to spin crossover in the temperature interval 70—140 K, was associated[13] with a transition of the coordinated O atom of the nitroxyl fragment from axial to equatorial position in the heterospin cyclic dimer. A structurally similar $Cu(hfac)_2$ tetranuclear complex with 3-pyridyl-substituted iminonitroxyl exhibits a two-step

Published in Russian in *Izvestiya Akademii Nauk. Seriya Khimicheskaya,* No. 11, pp. 2304—2325, November, 2004.

transition at 140—152 K and 70—80 K (both steps with hysteresis).[14] The high-temperature transition was treated[14] as a pseudospin transition because the magnetic effect was attributed to the change in the coordination of the imine N atom at the exocyclic Cu^{2+} ion in the square pyramid from equatorial to axial. It was also reported that the transition temperatures do not change after multiple cooling/heating cycles and on variation of the magnetic field strength. The results of quantum-chemical calculations substantiated the general considerations used to explain the reasons for the effects similar to spin crossover in the copper(II) complexes with nitroxyl radicals.[14,15] The magnetic effect similar to spin crossover with a narrow hysteresis loop was also recorded at 44—50 K in studies of the trinuclear $Cu(hfac)_2$ complex with dinitroxyl.[16] The crystal structures of the three complexes mentioned above were established at room temperature, *i.e.*, above the spin transition temperature. At temperatures below the transition temperature, the crystal structure of only one complex was established using some model approximations.[13,15] The reason is evident, that is, significant structural rearrangements in the complex usually lead to breakdown of the crystal.[13,14] However, structure determination below the transition temperature is necessary for detailed analysis of the structural changes responsible for the spin transitions. Noteworthy are also changes in the χT parameter of a chain complex of $Cu(hfac)_2$ with nitronylnitroxyl biradical.[17] Here, the χT value slowly decreased as temperature decreased from 100 to 30 K and then increased. The unusual effect undoubtedly deserved a separate investigation but the authors failed to study the crystal structure of this complex below the transition point because single crystals exploded at temperatures below 30 K.[17] Clearly, this behavior of the experimental dependence $\chi T(T)$ for the complex $Cu(hfac)_2$ with nitronylnitroxyl biradical has nothing in common with the classical spin crossover. However, we believe that all the magnetic effects reported in the literature[13—17] are of the same nature; from this point on we will call them "spin transition in non-classical systems".

In studying the complexes $Cu(hfac)_2L^R$ (L^R is a nitronylnitroxyl radical containing a pyrazole substituent at position 2 of imidazole ring) we obtained a family of heterospin complexes that can exhibit the effects similar to spin crossover at relatively high temperatures (130—230 K).[15,18,19] In most cases, single crystals of these complexes retained their quality in the temperature range covering the structural phase transition and the corresponding magnetic transition. The structures of all heterospin complexes and solid solutions based on them were established at temperatures below and above the magnetic transition temperature. This provided a unique possibility for the structural dynamics of these systems to be followed in the phase transition region. Despite considerable changes in the unit cell volumes on repetition of the cooling/heating cycles, compression and expansion of some single crystals appeared to be reversible.

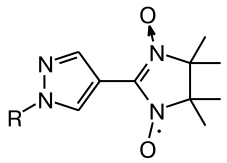

L^R

(R = Me, Et, Pr^n, Pr^i, Bu^n)

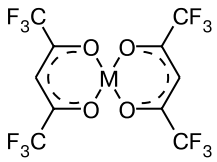

$M(hfac)_2$

(M = Cu, Mn, Ni, Co)

We found that in the solid phase all the compounds exhibiting the magnetic effects similar to spin crossover have a chain polymeric structure because of the bidentate-bridging coordination of paramagnetic ligands.[18] Phase transitions without breakdown of crystals are rare to occur in these structures because polymorphous transformations of a single crystal without loss of quality require a large number of cooperative motions of (i) fragments inside the polymer chains and (ii) the entire polymer chains inside the crystal. Multiple repetition of cooling/heating cycles causes a repeated anisotropic expansion and compression of crystals. We called these mechanically stable crystals "breathing" crystals.[20,21] The results of synthetic and structural dynamics studies of the "breathing" crystals have attracted the attention of researchers working not only in the field of design of molecule-based magnets but also in the field of research on the phase transitions, polymorphous transformations of polymers, and problems of solid-state physics and mechanical stability of crystals.[22] This gave an impetus to our efforts to summarize the most important results obtained in our studies on the spin transitions in non-classical systems.

Diversity of magneto-structural anomalies

First of all, we would like to draw the reader´s attention to diversity of possible manifestations of magnetic anomalies (judging from the character of the temperature dependences of μ_{eff} or χT) in the compounds where non-classical spin transitions can occur. The $\mu_{eff}(T)$ dependence obtained for complex $Cu(hfac)_2L^{Me}$ is shown in Fig. 1. The μ_{eff} jump occurs in a rather narrow temperature range and its character is much like that of the classical systems passing from the high-spin to the low-spin state. An abrupt decrease in μ_{eff} corresponds to a decrease in the effective magnetic moment of $Cu(hfac)_2L^{Me}$ by a factor of $\sqrt{2}$, which indicates that 50% of the spins ($S = 1/2$) in the sample disappeared. An explanation for this magnetic anomaly must first of all be looked for in structural rearrangement of the compound that occurs on temperature variation.

A single crystal study of $Cu(hfac)_2L^{Me}$ at 295 K showed that the compound has a chain polymeric structure due to

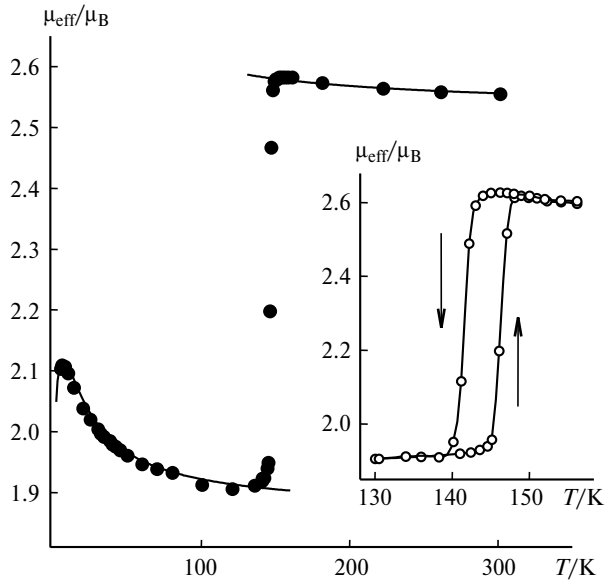

Fig. 1. Temperature dependence of μ_{eff} for $Cu(hfac)_2L^{Me}$.

the bridging coordination of L^{Me} through the imine atom N of pyrazole and one of the O atoms of the nitronyl-nitroxyl fragment (so-called "head-to-tail" chain motif, Fig. 2).[18] The environment of the Cu atom includes two hfac ligands (characterized by short distances $Cu—O_{hfac}$) in the equatorial plane and the O atom of NO group and the N atom of pyrazole heterocycle belonging to different bridging ligands L^{Me} in axial positions. The distance $Cu—O_L$ to the axial atom O of nitroxyl group is rather long (2.484 Å), which provides an explanation for the dominance of ferromagnetic exchange interaction in the exchange clusters $Cu^{2+}—O^{\bullet}—N<$.[14,23–25]

The shortest intra-chain and chain-chain distances between noncoordinated oxygen atoms of NO groups are long (at least 4.10 Å) and the shortest chain-chain contacts F...F are at least 2.92 Å. Therefore, exchange interactions between paramagnetic centers in $Cu(hfac)_2L^{Me}$ are located in the exchange clusters $Cu^{2+}—O^{\bullet}—N<$. Since at room temperature all coordination units CuO_5N containing the exchange clusters $Cu^{2+}—O^{\bullet}—N<$ in the structure of $Cu(hfac)_2L^{Me}$ contains are identical, the reason for "disappearance" of only 50% of spins could be clarified only after establishment of the crystal structure of the low-temperature phase (at $T < 140$ K).

However, single crystals of $Cu(hfac)_2L^{Me}$ cooled below the transition temperature causes are cracked. Nevertheless, in one experiment we succeeded in collecting a data array large enough to establish the crystal structure below the transition temperature (at 140 K). We found that cooling of the sample to 230±1 K is accompanied by irreversible transition of the monoclinic ("head-to-tail-1") polymorph of $Cu(hfac)_2L^{Me}$ into triclinic ("head-to-tail-2") polymorph. As a consequence, the crystallographically independent unit of the "head-to-tail-1" chain is doubled and the chain of the "head-to-tail-2" phase contains two types of Cu atoms, Cu(1) and Cu(2), with similar geometries of the coordination environment (Table 1). On further cooling the "head-to-tail-2" phase undergoes a reversible structural and the corresponding magnetic phase transition involving a change in the Jahn—Teller axis of the Cu bipyramids. Now in 50% of the coordination units CuO_5N the O atoms of nitroxyl groups and the N atoms of the pyrazole ring are displaced in equatorial positions with short distances $Cu—O_L$ and $Cu—N_L$ (1.992 and 2.014 Å, respectively, see Scheme 1), while two O atoms of the hfac ligands are displaced into axial positions. As a result, the bond lengths are shortened by 0.49 ($Cu—O_L$) and 0.32 Å ($Cu—N_L$).

Such great changes in the coordination bond lengths should be emphasized. In the other 50% of CuO_5N units the distances $Cu—O_L$ are much less shortened (by 0.035 Å) while the $Cu—N_L$ distances remain nearly unchanged within the limits of experimental error as temperature decreases to 140 K. In other words, at 140 K in these units the atoms O_L and N_L retain their axial positions while all equatorial positions are occupied by the O_{hfac} atoms separated from Cu atoms by nearly 2 Å.

Cooling of $Cu(hfac)_2L^{Me}$ samples is accompanied by intense crystal lattice dynamics. For instance, at room temperature the angle between the plane formed by the pyrazole ring atoms and the plane containing the atoms of the CN_2 unit of the $O^{\bullet}—N—C=N→O$ fragment of imidazole ring is ~13° for the "head-to-tail-1" and ~8° for the "head-to-tail-2" polymorph (see Table 1). At 140 K, in 50% of those bridging ligands L where O_L atoms change

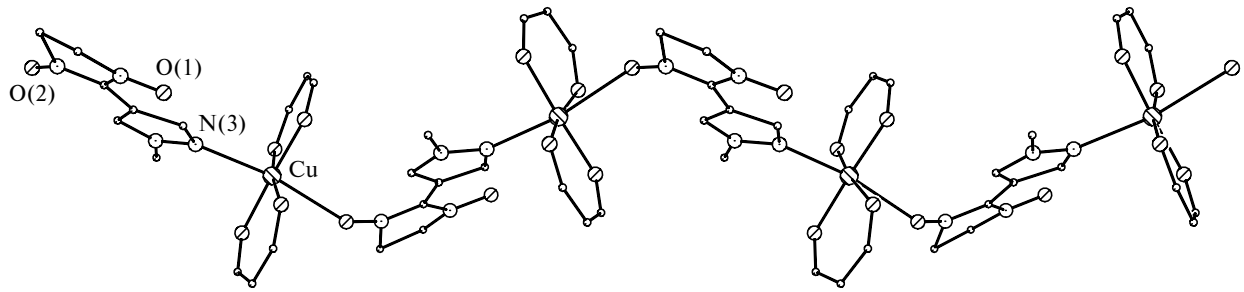

Fig. 2. "Head-to-tail"-type polymeric chain in the structure of $Cu(hfac)_2L^{Me}$.

Scheme 1

Irreversible transition of the "head-to-tail-1" polymorph into the "head-to-tail-2" polymorph and reversible transition between the low-temperature and high-temperature phases of the "head-to-tail-2" polymorph

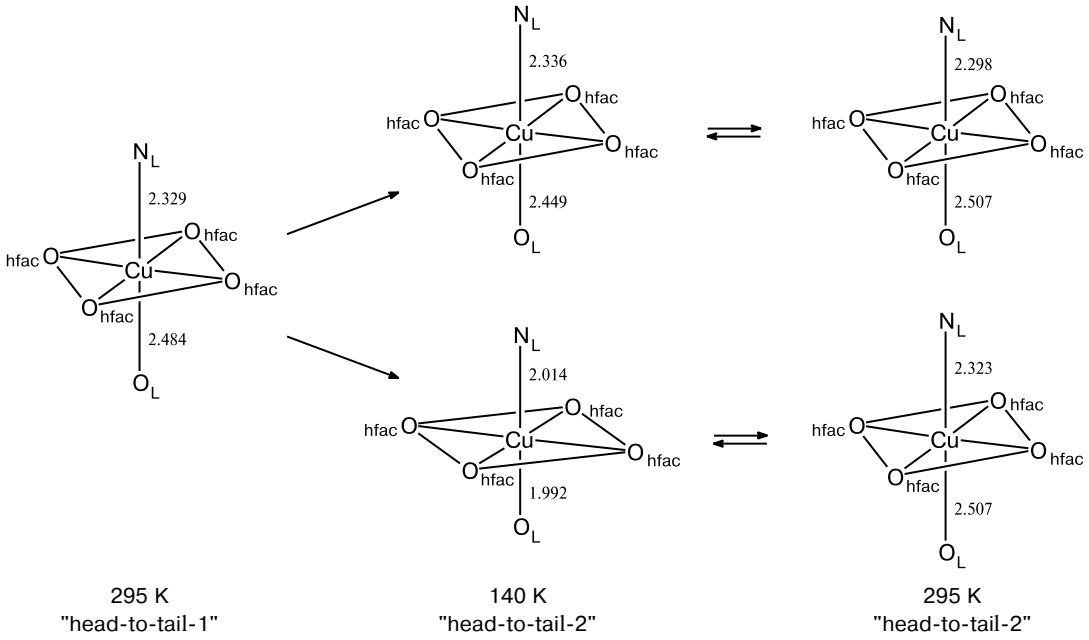

Table 1. Selected geometric parameters of crystal structures of the "head-to-tail-1" (I) (295 K) and "head-to-tail-1" (II) (295 K and 140 K) polymorphs of complex $Cu(hfac)_2L^{Me}$

Parameter	**I** ($P2_1/n$)*	**II** ($P\bar{1}$)*			
T/K	295	295	295	140	140
Central atom	Cu	Cu(1)	Cu(2)	Cu(1)	Cu(2)
Bond/Å					
Cu—O_L	2.484(5)	2.507(7)	2.507(6)	1.992(9)	2.449(9)
Cu—N_L	2.329(5)	2.323(7)	2.298(7)	2.014(10)	2.336(10)
Cu—O_{hfac}	1.936(4)	1.930(6)	1.937(6)	1.981(8)	1.936(9)
	1.950(4)	1.942(6)	1.947(6)	2.003(9)	1.937(9)
	1.956(4)	1.946(6)	1.959(7)	2.257(9)	1.966(9)
	1.962(4)	1.964(6)	1.968(6)	2.290(8)	1.976(9)
Angle/deg					
CN_2—Pz	13.3(6)	7.8(1.5)	8.6(1.2)	1.4(1.5)	11.3(1.7)

* Space group.

their positions from axial to equatorial in the coordination polyhedron this angle substantially decreases (to 1.4°), whereas in the other 50% of the ligands L whose O_L atoms retain their axial positions it changes to a much lesser extent (to 11.3°). However, despite the fact that these cooperative dynamic processes involve the whole single crystal, we will not dwell on them because they occur "far" from the exchange clusters Cu^{2+}—O•—N<, which are more important for elucidation of correlations between the magnetic properties and structure of compound at the microscopic level.

Changes occurring in the structure of $Cu(hfac)_2L^{Me}$ crystals on cooling from 293 to 140 K (see above) provide a clear explanation for the features of the experimental dependence $\mu_{eff}(T)$ obtained for this compound (see Fig. 1). Since at room temperature oxygen atoms in all coordination units CuO_5N occupy axial positions, we deal with ferromagnetic exchange interactions in the exchange clusters Cu^{2+}—O•—N< (particular numerical values of the exchange integrals obtained using the approach[26] can be found in the literature[18,19]) responsible for a smooth increase in μ_{eff} in the high-temperature range (300—170 K). The same is also observed for the low-temperature phase in the temperature range 80—10 K. In the transition region the number of spins in the solid phase of $Cu(hfac)_2L^{Me}$ is halved. This is due to displacement of coordinated atoms O_L of nitroxyl groups from axial to equatorial positions in 50% of CuO_5N units. As a result, weak ferromagnetic interaction in the exchange clusters Cu^{2+}—O•—N< in these units changes to strong antiferromagnetic interaction resulting in spin compensation.

The polymer chain structure of $Cu(hfac)_2L^{Pr^n}$ and the lengths of the distances Cu—O_L and Cu—N_L in the coordination units at different temperatures are shown in Fig. 3. In the solid phase the polymer chains of $Cu(hfac)_2L^{Pr^n}$ have a "head-to-head" motif, which leads to the formation of alternating coordination units CuO_6 and CuO_4N_2.

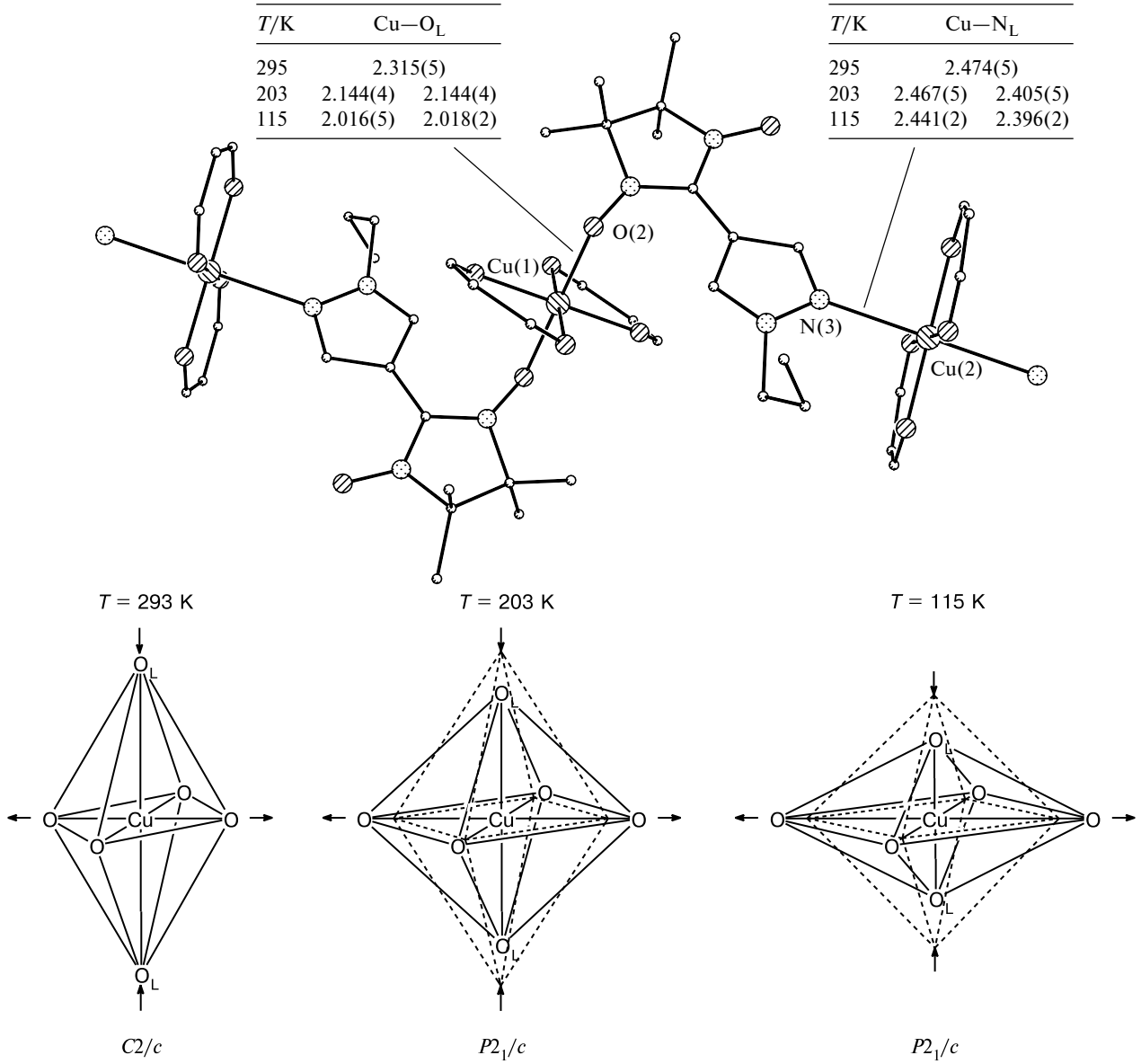

Fig. 3. "Head-to-head"-type chain in the structure of $Cu(hfac)_2L^{Pr^n}$ and the structural dynamics of coordination units at different temperatures.

The CuO_6 units contain heterospin exchange clusters >N—˙O—Cu^{2+}—O˙—N<. Changes in the bond lengths in these clusters on cooling are responsible for the behavior of the $\mu_{eff}(T)$ dependence. Considerable shortening of the distances between Cu atoms and coordinated oxygen atoms (Cu—O_L) in the CuO_6 units is accompanied by an increase in the Cu—O_{hfac} distance in the CuO_6 units along the O_{hfac}—Cu—O_{hfac} "axis" by 0.144 and 0.155 Å at 203 K and by an additional 0.144 and 0.133 Å at 115 K. In fact, we deal with replacement of the O_L—Cu—O_L "axis of octahedron" elongated at room temperature (on cooling it is shortened by 0.598 Å) by the O_{hfac}—Cu—O_{hfac} "axis" elongated at low temperature (on cooling it is lengthened by 0.576 Å) in distorted Jahn—Teller octahedral units CuO_6. However, between 293 and 115 K (*e.g.*, at 203 K), when the O_L—Cu—O_L "axis" is only partially shortened and the O_{hfac}—Cu—O_{hfac} "axis" is only partially lengthened, the CuO_6 units are transformed into flattened octahedra that are rare in occurrence.[18,27] The phase transition also causes the symmetry of the crystal to be changed (see Fig. 3).

Thus, structural rearrangements of the coordination units CuO_6 reflect displacement of coordinated O atoms of the nitroxyl groups >N—˙O from axial to equatorial positions, which gives rise to strong antiferromagnetic interaction in the clusters >N—˙O—Cu^{2+}—O˙—N<. Therefore, at $T \leq 230$ K a smooth decrease in μ_{eff} of $Cu(hfac)_2L^{Pr^n}$ on cooling is followed by a rapid decrease

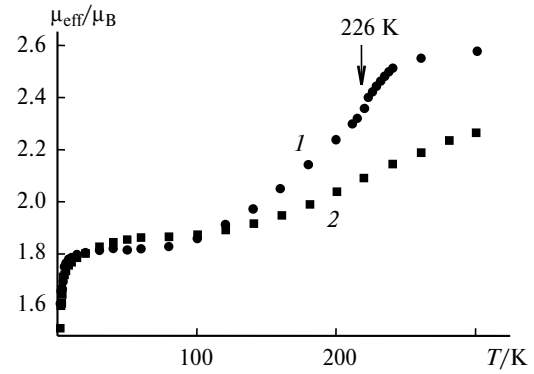

Fig. 4. Temperature dependences of μ_{eff} for $Cu(hfac)_2L^{Pr^n}$ (*1*) and $Cu(hfac)_2L^{Pr^i}$ (*2*).

of the $\mu_{eff}(T)$ curve which reaches a plateau characterized by $\mu_{eff} \approx 1.8\ \mu_B$ (Fig. 4), being indicative of a dramatic strengthening of antiferromagnetic interactions in the exchange clusters >N—˙O—Cu^{2+}—O˙—N< below the structural phase transition at 226 K. The decrease in μ_{eff} to $1.8\ \mu_B$ shows that 50% of spins in $Cu(hfac)_2L^{Pr^n}$ "disappear" on cooling to 50 K. This is in excellent agreement with the decrease in the spin of the exchange cluster >N—˙O—Cu^{2+}—O˙—N< to S = 1/2. At $T < 50$ K, only the remaining spins of the exchange clusters and the spins of the Cu^{2+} ions in the CuO_4N_2 units contribute to the magnetic moment of $Cu(hfac)_2L^{Pr^n}$. This is the reason for the decrease in μ_{eff} by a factor of $\sqrt{2}$ at ~50 K compared to the μ_{eff} value at room temperature.

The polymer chain motifs in $Cu(hfac)_2L^{Pr^i}$ and $Cu(hfac)_2L^{Pr^n}$ crystals are identical (see Fig. 3).[19] However, a unique structural feature of $Cu(hfac)_2L^{Pr^i}$ is that at room temperature the CuO_6 units are flattened octahedra, which is rare in occurrence for copper(II) complexes. The equatorial distances Cu—O_{hfac} and Cu—O_L are 2.130 and 2.143 Å, respectively (*cf.* 1.975 Å for the axial distances Cu—O_{hfac}). On cooling of $Cu(hfac)_2L^{Pr^i}$ crystals the bond lengths and bond angles in the ligands (L^{Pr^i} and hfac) remain nearly unchanged. The CuO_4N_2 units are characterized by minor shortening of axial distances Cu—N_L by ~0.05 Å and the CuO_6 flattened octahedra are transformed into elongated ones because appreciable shortening of the Cu—O_L distance (2.143→2.002 Å) is accompanied by simultaneous lengthening of two Cu—O_{hfac} distances (2.130→2.293 Å). Therefore, in the temperature range 293—123 K the atoms O_L always occupy equatorial positions irrespective of structural rearrangement of the CuO_6 unit of $Cu(hfac)_2L^{Pr^i}$. Figure 5 schematically depicts the rearrangement of the CuO_6 units (the number of these units equals half the total number of the coordination units in infinite chain).

The structural dynamics of $Cu(hfac)_2L^{Pr^i}$ in the temperature interval 123—293 K is quite similar to that of $Cu(hfac)_2L^{Pr^n}$ in the temperature range 115—203 K (*i.e.*, below the structural phase transition in $Cu(hfac)_2L^{Pr^n}$). This suggests that the transition temperature of $Cu(hfac)_2L^{Pr^i}$ exceeds 293 K. Unfortunately, attempts to transform the CuO_6 flattened octahedra into elongated ones by heating $Cu(hfac)_2L^{Pr^i}$ failed because decomposition of the complex began at 325 K. Would $Cu(hfac)_2L^{Pr^i}$ be thermally stable, elongation of the Cu—O_L distances and the formation of elongated octahedral units CuO_6 with lengthened Cu—O_L distances could be expected with an increase in temperature. In this case the μ_{eff} value for $Cu(hfac)_2L^{Pr^i}$ must tend to a value of the order of 2.5—2.6 μ_B similarly to μ_{eff} of $Cu(hfac)_2L^{Pr^n}$. On cooling the μ_{eff} value for $Cu(hfac)_2L^{Pr^i}$ tends to the limiting value of 1.8 μ_B similarly to $Cu(hfac)_2L^{Pr^n}$ (see Fig. 4).

The polymer chain motif and packing in the solid phase of $Cu(hfac)_2L^{Bu^n} \cdot 0.5C_6H_{14}$ are the same as those of $Cu(hfac)_2L^R$ (R = Pr^n, Pr^i) (Fig. 6, *a*). However, the structural dynamics of the coordination units in

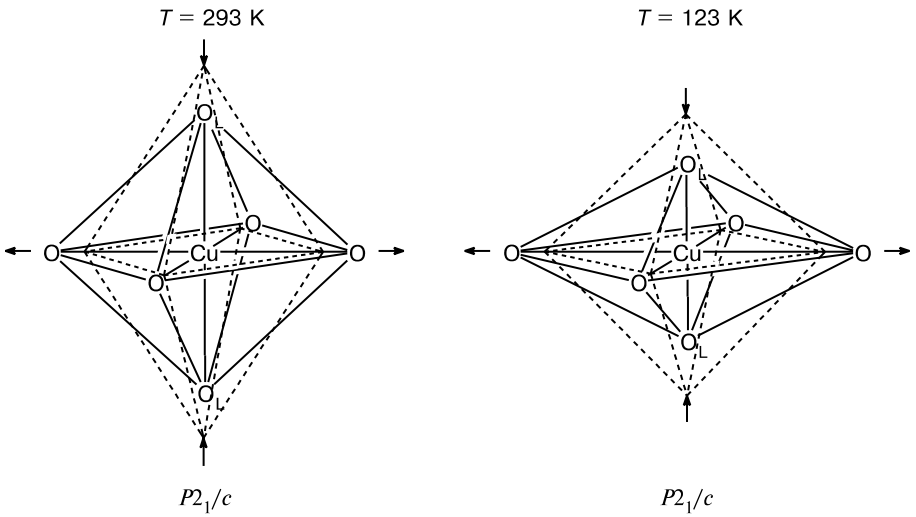

Fig. 5. Scheme of compression of the CuO_6 coordination units in the structure of $Cu(hfac)_2L^{Pr^i}$.

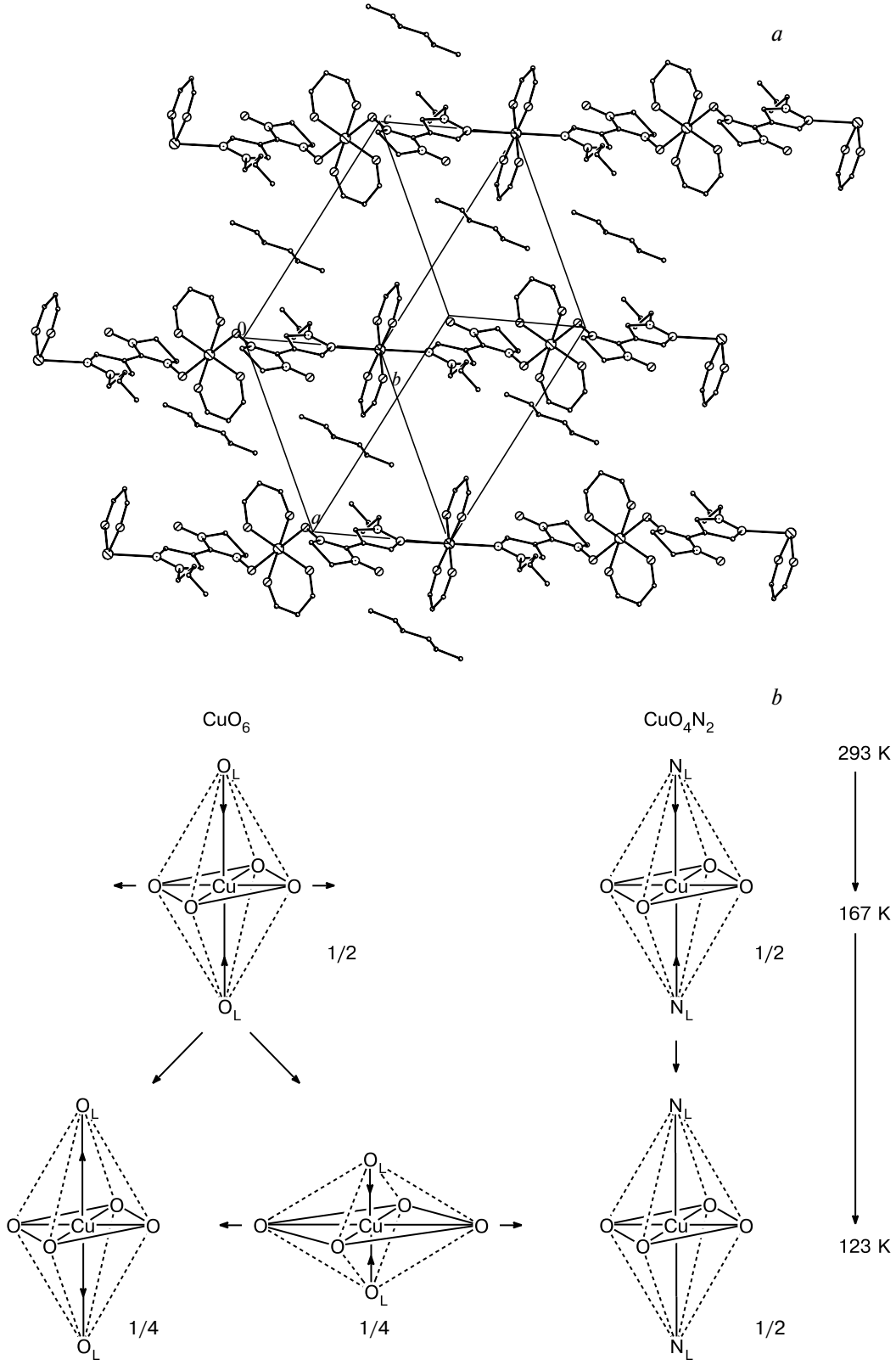

Fig. 6. Polymeric chain packing (*a*) and structure rearrangement scheme of coordination polyhedra (*b*) in the structure of $Cu(hfac)_2L^{Bu^n} \cdot 0.5C_6H_{14}$.

$Cu(hfac)_2L^{Bu^n} \cdot 0.5C_6H_{14}$ on cooling has little in common with the dynamics of $Cu(hfac)_2L^R$ ($R = Pr^n$, Pr^i).

The structure of $Cu(hfac)_2L^{Bu^n} \cdot 0.5C_6H_{14}$ was established at 295, 171, 167, and 123 K. At room temperature, all CuO_6 units are elongated octahedra with the Cu—O_L and Cu—O_{hfac} distances of 2.320 Å and 1.970—1.983 Å, respectively. The coordination polyhedra of Cu atoms in the CuO_4N_2 units have a similar shape, being characterized by rather long Cu—N_L distances (2.514 Å) and much shorter Cu—O_{hfac} distances (1.937—1.977 Å). As temperature decreases to 167 K, the Cu—O_L distance is shortened from 2.320 to 2.250 Å. Similarly to $Cu(hfac)_2L^{Pr^i}$, structural rearrangements manifest themselves as a decrease in the unit cell volume by ~4% and small variation of the lattice parameters. Further cooling to 123 K leads to a doubling of unit cell volume because the independent part of the structure is doubled. The coordination units CuO_4N_2 in $Cu(hfac)_2L^{Bu^n} \cdot 0.5C_6H_{14}$ adopt a pseudocentral symmetry with different Cu—N_L distances (2.457 and 2.468 Å). The CuO_6 units retain central symmetry but can now be divided into two types. One type is characterized by a dramatic increase in the axial distances Cu—O_L (2.250→2.348 Å). The other type is characterized by abrupt shortening of the Cu—O_L distances (2.250→2.007 Å), resulting in displacement of O_L atoms in these units to equatorial positions and to displacement of two O_{hfac} atoms to axial positions (2.023→2.240 Å) (Table 2). By and large, the unit cell volume of the $Cu(hfac)_2L^{Bu^n} \cdot 0.5C_6H_{14}$ single crystal decreases by 5.7% on cooling from 295 to 123 K. Structural rearrangement of CuO_6 units in $Cu(hfac)_2L^{Bu^n} \cdot 0.5C_6H_{14}$ single crystal on cooling is schematically shown in Fig. 6, *b*.

At 163 K, $Cu(hfac)_2L^{Bu^n} \cdot 0.5C_6H_{14}$ undergoes a structural phase transition.[19] As a result, the Cu—O_L distances in 50% of exchange clusters >N—$^{\bullet}$O—Cu^{2+}—O$^{\bullet}$—N<

Table 2. Changes in the bond lengths (*d*) in the CuO_6 and CuO_4N_2 coordination units in the structure of $Cu(hfac)_2L^{Bu^n} \cdot 0.5C_6H_{14}$ at different temperatures

Coordination unit	Bond	*d*/Å			
		295 K	171 K	167 K	123 K
CuO_6	Cu—O_L	2.320(3)	2.251(4)	2.250(3)	2.007(2)
					2.348(2)
	Cu—O_{hfac}	1.970(2)	1.975(3)	1.976(3)	2.031(2)
		1.983(2)	2.023(3)	2.023(3)	2.240(2)
					1.960(2)
					1.969(2)
CuO_4N_2	Cu—N_L	2.514(3)	2.469(4)	2.470(4)	2.457(3)
					2.468(3)
	Cu—O_{hfac}	1.937(2)	1.980(3)	1.983(3)	1.943(2)
		1.977(2)	1.938(3)	1.943(3)	1.945(2)
					1.986(2)
					1.991(2)

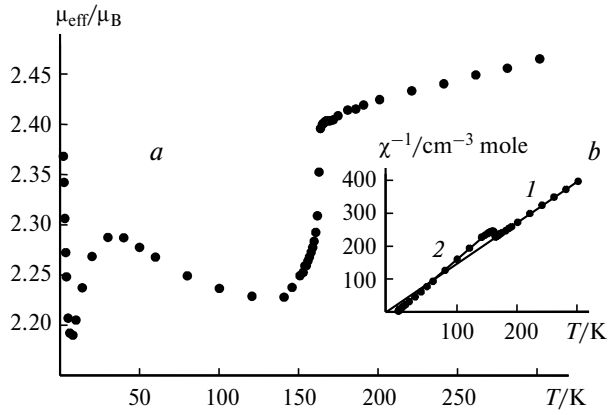

Fig. 7. Temperature dependences of μ_{eff} (*a*) and inverse magnetic susceptibility (*b*) for $Cu(hfac)_2L^{Bu^n} \cdot 0.5C_6H_{14}$.

are shortened from 2.32 Å to ~2.00 Å (see Table 2 and Fig. 6). This gives rise to a strong antiferromagnetic interaction between the unpaired electrons of Cu^{2+} ions and N—$^{\bullet}$O groups in these spin triads. As a result, the effective spin of this group decreases to 1/2, thus being responsible for the abrupt decrease in μ_{eff} at 163±2 K (Fig. 7). In the other 50% of exchange clusters >N—$^{\bullet}$O—Cu^{2+}—O$^{\bullet}$—N< the Cu—O_L distances increase from 2.32 to 2.35 Å, which causes the sign of exchange interaction to be changed from negative to positive. As a consequence, the decrease in μ_{eff} on cooling from 300 to 165 K is changed by an increase in this parameter at T <150 K, *i.e.*, below the transition region (see Fig. 7). The Curie—Weiss equation parameters for the regions 1 and 2 are $C_1 = 0.805$, $\theta_1 = -19$ K and $C_2 = 0.625$, $\theta_2 = 0.3$ K, respectively. Since the parameters C_1 and C_2 are proportional to the number of paramagnetic centers, the decrease in C_2 compared to C_1 is a direct evidence of "disappearance" of a portion of paramagnetic centers in the exchange clusters >N—$^{\bullet}$O—Cu^{2+}—O$^{\bullet}$—N< in which strong antiferromagnetic interactions occur. A C_2/C_1 ratio of 0.78 is similar to a value of 0.75 corresponding to complete pairing of two spins inside the clusters mentioned above. Thus, the character of the $\mu_{eff}(T)$ plot observed for $Cu(hfac)_2L^{Bu^n} \cdot 0.5C_6H_{14}$ is in excellent agreement with the structural dynamics of the heterospin complexes under study on cooling.

Consider some differences in chain packing in the "head-to-head" chain complexes discussed above. For instance, the chain structure of $Cu(hfac)_2L^{Pr^i}$ (or $Cu(hfac)_2L^{Pr^n}$) is such that the shortest distances between fluorine atoms are at least 3.12 Å. Hexane molecules present in the structure of $Cu(hfac)_2L^{Bu^n} \cdot 0.5C_6H_{14}$ pull chains apart (see Fig. 6, *a*), thus making the F...F contacts longer (3.21 Å). Comparison of these chain—chain contacts F...F with the sum of the Van der Waals radii of two F atoms (2.80 Å) shows that complexes $Cu(hfac)_2L^R$ have rather "loose" structures. In principle, we can as-

sume that the crystals of $Cu(hfac)_2L^R$ can be compressed on cooling due to shortening of the F...F contacts. However, an X-ray diffraction study of $Cu(hfac)_2L^R$ at different temperatures revealed an opposite situation. As mentioned above, a decrease in temperature has the most pronounced effect on the bond lengths in the coordination polyhedra, the chain—chain contacts between O atoms of nitroxyl groups are also shortened by 0.2—0.3 Å; the angles between the heterocycle planes can also change. In this case, the chain—chain contacts F...F in $Cu(hfac)_2L^R$ (R = Pr^n, Pr^i, Bu^n) remain nearlly unchanged. Expectations of changes in these contacts in the "head-to-tail" structure of $Cu(hfac)_2L^{Me}$ for which the shortest contacts F...F (2.92 Å) at room temperature are similar to the sum of the Van der Waals radii of two fluorine atoms would be even more strange. By this we again emphasize that the greatest structural rearrangement occurring in the course of the phase transition in $Cu(hfac)_2L^R$ involves the coordination units.

The structural and magnetic properties of $Cu(hfac)_2L^{Et}$ deserve particular consideration. Similarly to $Cu(hfac)_2L^R$ (R = Pr^n, Pr^i, Bu^n), the solid phase of this compound is formed by the "head-to-head" arranged polymer chains (Fig. 8). The most important structural features of $Cu(hfac)_2L^{Et}$ at 293 K are very short distances Cu—O_L (2.237 Å) and Cu—N_L (2.375 Å) in centrally symmetrical, crystallographically independent units CuO_6 and CuO_4N_2, respectively. As temperature decreases, the distances Cu—O_L in the CuO_6 units increase (Table 3). The Cu—O_{hfac} distances in the CuO_6 units are also changed. Lengthening of axial distances along the O_L—Cu—O_L "axis" is accompanied by a comparable (~0.043 Å) shortening of each Cu—O_{hfac} bond along one O_{hfac}—Cu—O_{hfac} "direction". In fact, at 188 K we deal with a change in the arrangement of the long axis of the Cu-bipyramid in the CuO_4N_2 units, namely, the coordinated N atoms of pyrazole heterocycles now occupy equatorial positions (d(Cu—N_L) 2.375→2.079 Å), thus displacing two O_{hfac} atoms to axial positions (d(Cu—O_{hfac}) 1.996→2.269 Å). Further cooling is accompanied by shortening of the Cu—N_L distances in the CuO_4N_2 units and by lengthening of the Cu—O_L distances in the CuO_6 units. Thus, we can say that almost all structural changes in the solid phase of $Cu(hfac)_2L^{Et}$ on cooling occur in the CuO_6 and CuO_4N_2 coordination units because the angles and distances in the coordinated hfac anions and L^{Et} remain unchanged within the limits of experimental error. Moreover, these parameters of coordinated ligand L^{Et} coincide with those of a free ligand.

Table 3. Changes in the bond lengths (d) in the CuO_6 and CuO_4N_2 coordination units in the structure of $Cu(hfac)_2L^{Et}$ at different temperatures

Coordination bond	Bond	d/Å		
		295 K	188 K	115 K
CuO_6	Cu—O_L	2.237(4)	2.260(3)	2.281(3)
	Cu—O_{hfac}	2.028(5)	2.007(4)	1.985(4)
		1.965(4)	1.960(4)	1.958(4)
CuO_4N_2	Cu—N_L	2.375(5)	2.079(4)	2.055(4)
	Cu—O_{hfac}	1.979(4)	1.973(4)	1.961(4)
		1.996(4)	2.269(3)	2.313(3)

The temperature dependence of the effective magnetic moment of $Cu(hfac)_2L^{Et}$ has a complex and quite unusual fashion (Fig. 9). At room temperature, the μ_{eff} value is similar to a theoretical value of 2.45 μ_B calculated per {$Cu(hfac)_2L^{Et}$} unit of a system of nearly noninteracting Cu^{2+} ion and nitroxyl spins. On cooling to ~225 K the μ_{eff} value gradually decreases to ~2.3 μ_B. The short Cu—O_L distance (2.237 Å) in octahedral CuO_6 units is the reason for predominance of antiferromagnetic con-

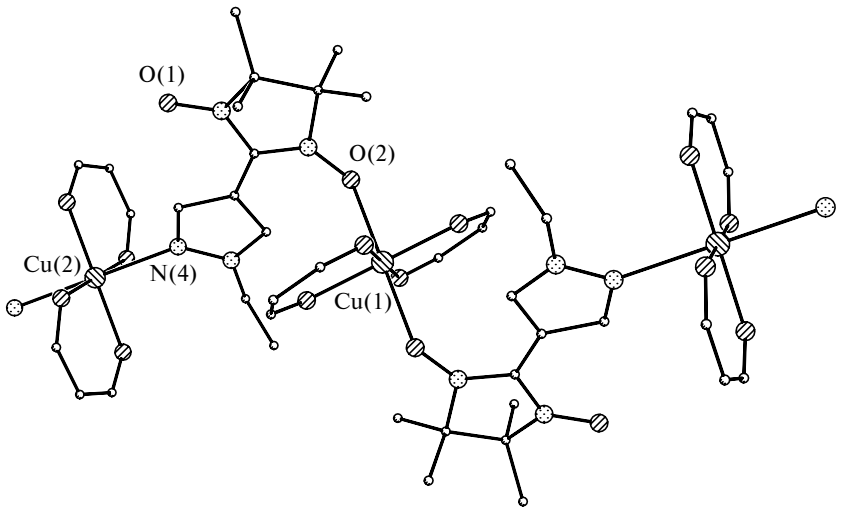

Fig. 8. "Head-to-head"-type polymeric chain in the structure of $Cu(hfac)_2L^{Et}$.

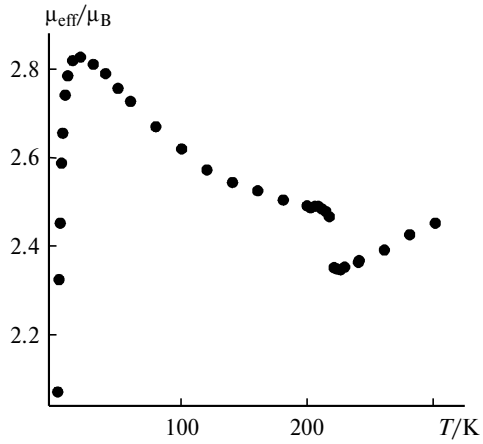

Fig. 9. Temperature dependence of μ_{eff} for $Cu(hfac)_2L^{Et}$.

tribution to the exchange clusters >N—˙O—Cu^{2+}—O˙—N< in the temperature interval 225—300 K (the sign of exchange interaction is known to be very sensitive to the length of the Cu—O_L distance).[14,23] The results of a structural study[18] of $Cu(hfac)_2L^{Et}$ below the transition point show that at 188 K the distance Cu—O_L in the CuO_6 units increases by only ~0.02 Å. This minor bond elongation causes a dramatic weakening of the antiferromagnetic contribution and predominance of ferromagnetic interactions in the exchange clusters >N—˙O—Cu^{2+}—O˙—N<, the type of exchange being changed jumpwise at 220 K (see Fig. 9). Subsequent cooling accompanied by further increase in the Cu—O_L distance (see above) has no effect on the type of exchange interaction in the clusters >N—˙O—Cu^{2+}—O˙—N<, which remains ferromagnetic in character, being responsible for the increase in μ_{eff} down to ~25 K. Below this temperature the μ_{eff} value rapidly decreases owing to manifestation of antiferromagnetic intermolecular interactions. The jumpwise increase in μ_{eff} at temperatures below 220 K is a quite unusual phenomenon that could never be observed for spin transitions in the classical systems. Indeed, in the case where two or more paramagnetic centers contribute to the total spin of the exchange cluster, various situations become possible.

1. Structural phase transition changes the type of exchange interaction from ferromagnetic to antiferromagnetic (in, *e.g.*, $Cu(hfac)_2L^{Me}$) or the energy of antiferromagnetic interaction abruptly increases as is the case of $Cu(hfac)_2L^{Pr^n}$. Here, the μ_{eff} value decreases jumpwise at the transition temperature. This magnetic behavior of the compound is similar to spin transitions in classical systems in character of the dependence $\mu_{eff}(T)$.

2. Structural phase transition changes the type of the interaction between the unpaired electrons in the exchange cluster from antiferromagnetic to ferromagnetic ($Cu(hfac)_2L^{Et}$). Here, the μ_{eff} value increases jumpwise at the transition temperature. This character of the dependence $\mu_{eff}(T)$ is impossible in the case of spin transitions in classical systems.

3. Structural phase transition is such that situation 1 occurs in a fraction of the exchange clusters and situation 2 simultaneously occurs in the remaining exchange clusters (the case of $Cu(hfac)_2L^{Bu^n}$). Here, at the transition point the μ_{eff} value decreases jumpwise and then increases. This magnetic behavior of the compound (shape of the dependence $\mu_{eff}(T)$) is also impossible in the case of spin transitions in classical systems.

Thus, the results presented in this Section illustrate the variety of patterns of the $\mu_{eff}(T)$ dependence for the magnetic anomalies accompanying structural rearrangement of multicenter exchange clusters. It is no wonder that structural changes that mainly occur within the coordination polyhedra containing the exchange clusters are strongly affected by the structure of substituent R (R = Me, Et, Pr^n, Pr^i, Bu^n) in the paramagnetic ligand L^R which is not a constituent of the coordination unit. Since the effects similar to spin crossover belong to cooperative phenomena and each crystal of a compound under study "works" as one species, compounds with different compositions and, hence, packing exhibit different temperature dependences of μ_{eff}. *Vice versa*, a similar shape of the $\mu_{eff}(T)$ dependences for different compounds exhibiting spin transitions is an indication of minor disturbances that come from structure variation of paramagnetic molecules. All the $Cu(hfac)_2L^R$ (R = Me, Et, Pr^n, Pr^i, Bu^n) compounds discussed above exhibit different-shape dependences $\mu_{eff}(T)$. Only for $Cu(hfac)_2L^{Pr^n}$ and $Cu(hfac)_2L^{Pr^i}$ we can say that these compounds are similar in the sense of a general trend of changes in the dependence $\mu_{eff}(T)$.

Problem: wide variety of products

In the previous Section of this review we considered only those compounds that form solid phases with a polymeric chain structure at a 1 : 1 $Cu(hfac)_2/L^R$ ratio. Therefore, it may appear that reactions of $Cu(hfac)_2$ with organic paramagnetics L^R result in the only complex with particular composition and structure. However, this is not nearly so, being the main problem in developing methods of synthesis of the heterospin compounds that can exhibit magnetic effects called the spin transitions in non-classical systems. For instance, in studies of products of the reaction of $Cu(hfac)_2$ with the spin-labeled pyrazole L^{Me} we isolated a family of twelve compounds differing in composition and/or structure of the solid phase.[28] These compounds can be formed simultaneously, so the only way is to obtain them as high-quality single crystals and then separate mechanically. This is a necessary step because minor changes in the structure of the solid phase of the heterospin complex can strongly change its magnetic properties.

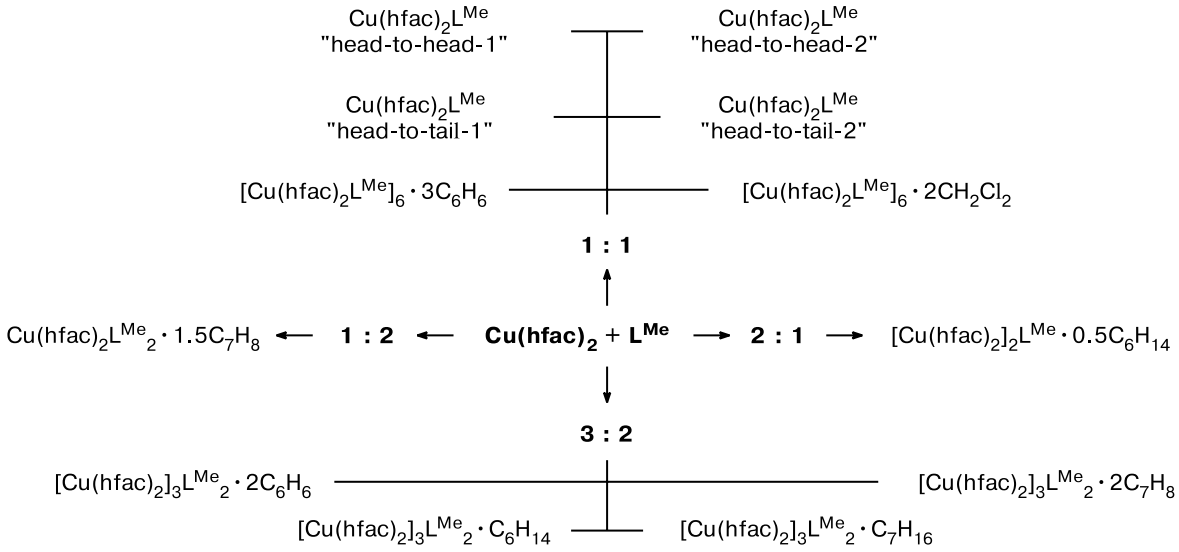

Fig. 10. Stoichiometry of the solid phases obtained in the reactions of $Cu(hfac)_2$ with L^{Me}.

These compounds can be divided into four groups with respect to the $Cu(hfac)_2 : L^{Me}$ ratio (Fig. 10). Note that four phases with a 1 : 1 $Cu(hfac)_2/L^{Me}$ ratio are polymorphs (to obtain the fifth polymorph, one should remove the solvate molecules from $[Cu(hfac)_2L^{Me}]_6 \cdot 3C_6H_6$ and $[Cu(hfac)_2L^{Me}]_6 \cdot 2CH_2Cl_2$). The crystal and molecular structures of all the twelve compounds were established.[28] The "head-to-tail-1" chain motif of $Cu(hfac)_2L^{Me}$ is shown in Fig. 2. The "head-to-tail-2" polymorph (see above) differs in the presence of two different coordination units CuO_5N owing to reduction of symmetry and the corresponding doubling of the crystallographically independent part of the structure. The "head-to-head-1" and "head-to-head-2" chain motifs are similar to those of, *e.g.*, $Cu(hfac)_2L^{Pr}$ (see Fig. 3). Polymer chains in the "head-to-head-2" structure are characterized by considerably different $Cu—O_L$ distances in the CuO_6 coordination units (2.395 and 2.459 Å) and Cu—O—N angles (131.3 and 140.6°), which is not observed in the "head-to-head-1" structure. These structural differences are large enough for the "head-to-head-1" structure to exhibit the effects similar to spin crossover and for the "head-to-head-2" structure to be "silent". The molecular structures of other compounds, namely, mononuclear $Cu(hfac)_2L^{Me}_2 \cdot 1.5C_7H_8$, dinuclear $[Cu(hfac)_2]_2L^{Me} \cdot 0.5C_6H_{14}$, trinuclear $[Cu(hfac)_2]_3L^{Me}_2 \cdot 2C_6H_6$, $[Cu(hfac)_2]_3L^{Me}_2 \cdot C_6H_{14}$, $[Cu(hfac)_2]_3L^{Me}_2 \cdot C_7H_{16}$ and $[Cu(hfac)_2]_3L^{Me}_2 \cdot 2C_7H_8$, and hexanuclear $[Cu(hfac)_2L^{Me}]_6 \cdot 3C_6H_6$ and $[Cu(hfac)_2L^{Me}]_6 \cdot 2CH_2Cl_2$ are shown in Fig. 11. Without dwelling on the structural features of the mono- and polynuclear complexes, mention may be made that none of them exhibits specific magnetic anomalies.

The number of reaction products that are formed in the system $Cu(hfac)_2—L^{Et}$ is somewhat smaller compared to that formed in the system $Cu(hfac)_2—L^{Me}$. Depending on the reagent ratio and the solvent used, either the chain polymer $Cu(hfac)_2L^{Et}$ (see above) or solvates of trinuclear complex $[Cu(hfac)_2]_3L^{Et}_2$ (see Fig. 11, *c*) can be formed, the latter being compositionally and structurally similar to the solvates of trinuclear complex $[Cu(hfac)_2]_3L^{Me}_2$ (Fig. 12). The solid phase obtained by crystallization from benzene or toluene always contains trinuclear complexes irrespective of the starting reagent ratio due to the much lower solubility of these compounds in these solvents compared to $Cu(hfac)_2L^{Et}$. In this case the excess paramagnetic ligand remains in solution. The solid phase obtained by crystallization from heptane or hexane at a 3 : 2 $Cu(hfac)_2/L^{Et}$ ratio always contains a mixture of $[Cu(hfac)_2]_3L^{Et}_2 \cdot Solv$ crystals (dark-red plates or rhomboi) with a small amount of brown needle-shaped $Cu(hfac)_2L^{Et}$ crystals that can be mechanically separated. In this case, co-crystallization of $[Cu(hfac)_2]_3L^{Et}_2 \cdot Solv$ and $Cu(hfac)_2L^{Et}$ is not unusual because experiments showed that the solubility of $[Cu(hfac)_2]_3L^{Et}_2 \cdot Solv$ is little less than the solubility of $Cu(hfac)_2L^{Et}$ in hexane and heptane. At a 1 : 1 reagent ratio, $Cu(hfac)_2L^{Et}$ needles are mainly crystallized. Thus, the result of crystallization from hexane or heptane primarily depends on the starting reagent ratio because complexes $[Cu(hfac)_2]_3L^{Et}_2 \cdot Solv$ and $Cu(hfac)_2L^{Et}$ are very poorly soluble in unsaturated hydrocarbons, so cooling and subsequent storage of reaction mixtures leads to nearly quantitative isolation of solid products. Therefore, dissolution of any complex $[Cu(hfac)_2]_3L^{Et}_2 \cdot Solv$ in hexane (or heptane) followed by adding L^{Et} until a 1 : 1 mole ratio results in reproduc-

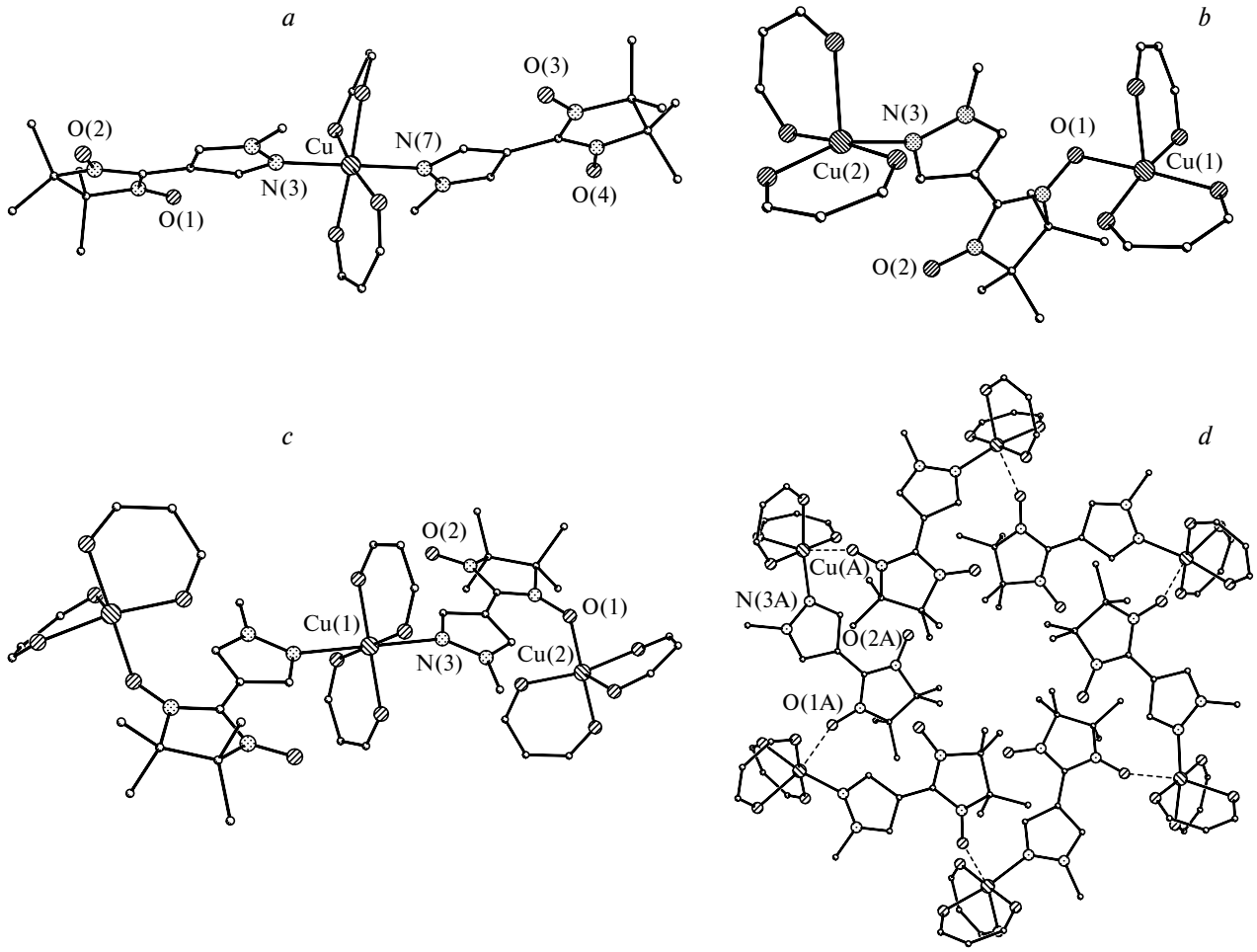

Fig. 11. Structures of mononuclear (*a*), dinuclear (*b*), trinuclear (*c*), and hexanuclear (*d*) complexes.

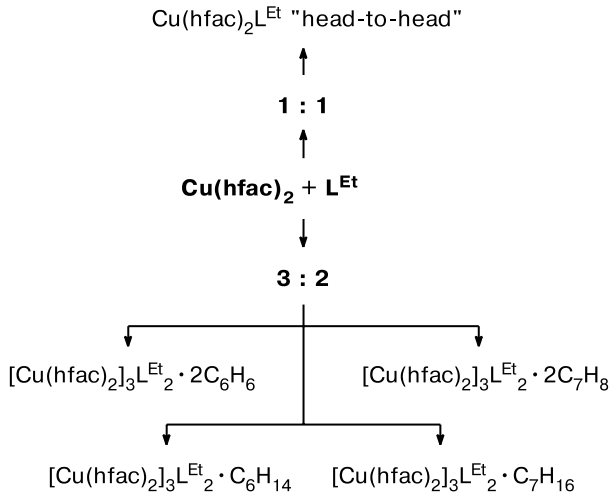

Fig. 12. Stoichiometry of the solid phases obtained in the reactions of $Cu(hfac)_2$ with L^{Et}.

ible formation of the "head-to-head" polymeric chain complex $Cu(hfac)_2L^{Et}$ (see Fig. 8). In contrast to $Cu(hfac)_2L^{Me}$, no formation of $Cu(hfac)_2L^{Et}$ polymorphs was observed; this made the study of solid solutions $Cu(hfac)_2L^{Me}{}_xL^{Et}{}_{1-x}$ (see below) much easier.

The examples given above show that reactions of $Cu(hfac)_2$ with L^R can result in heterospin complexes with different compositions and/or structures. Since often these compounds crystallize as mixtures of products, one should obtain them in the form of single crystals, mechanically separate the solid phases, and examine them by X-ray analysis. Particular attention should be paid to the cases where the crystals to be separated are similar in color and shape. Here, each (!) crystal of the compound under study must be checked by X-ray analysis prior to performing magnetic measurements.

Thus, a great variety of products with different compositions and structures can be formed in reactions of stereochemically nonrigid matrix $Cu(hfac)_2$, which is widely used in design of heterospin systems, with polyfunctional nitroxyls. It should be noted that only a few reaction products can possess unusual magnetic properties that deserve detailed investigation.

Solid solutions $M_xCu_{1-x}(hfac)_2L^{Et}$

The variety of complexes that can be formed in reactions of stereochemically nonrigid matrix $Cu(hfac)_2$ with nitroxyls can significantly complicate the search for compounds exhibiting magnetic anomalies (spin transitions in non-classical systems). However, once synthesized, these compounds provide additional possibilities for chemical modification of the physical effect. One method of chemical modification, which is widely used in studies of the STCS, involves formation of solid solutions of different metal compounds.[1,12]

A study of the magnetic anomaly of $Cu(hfac)_2L^{Et}$, namely, an abrupt increase in μ_{eff} on cooling below 220 K (see Fig. 9) attracted the greatest interest. This is a quite unusual effect; therefore, we studied[29] the possibility of formation of solid solutions $M_xCu_{1-x}(hfac)_2L^{Et}$ (M = Mn, Ni, Co). It was expected that Mn atoms must replace Cu atoms in the coordination units CuO_6 and Ni or Co atoms must replace Cu atoms in CuO_4N_2 units (Fig. 13). Series of $Mn_xCu_{1-x}(hfac)_2L^{Et}$, $Co_xCu_{1-x}(hfac)_2L^{Et}$, and $Ni_xCu_{1-x}(hfac)_2L^{Et}$ samples including single crystals of these compounds were synthesized. The results of X-ray diffraction studies of some single crystals confirmed our assumptions. Trends of changes in the $M—O_L$ and $M—N_L$ bond lengths in the $M_xCu_{1-x}(hfac)_2L^{Et}$ (M = Mn, Co) solid solutions (Table 4) are as follows: the $M—O_L$ distances in the MO_6 units are shortened with an increase in the mole fraction of Mn while the distances $M—N_L$ in the MO_4N_2 units remain the same as those in $Cu(hfac)_2L^{Et}$ (2.375 Å). A reverse situation was observed for $Co_xCu_{1-x}(hfac)_2L^{Et}$, namely, the increase in the mole fraction of Co is accompanied by gradual shortening of the $M—N_L$ distances in the MO_4N_2 units, whereas the $M—O_L$ distances in the MO_6 units remain unchanged, being equal to those in $Cu(hfac)_2L^{Et}$ (2.237 Å).

Preliminary X-ray diffraction studies proved that compounds $M(hfac)_2L^{Et}$ (M = Mn, Ni, Co) are isostructural to $Cu(hfac)_2L^{Et}$. Unlike the copper(II) compound, they do not tend to form different products in the reactions with L^R. This probably favored the formation of solid solutions $M_xCu_{1-x}(hfac)_2L^{Et}$ containing both the Jahn—Teller (Cu^{2+}) and non-Jahn—Teller ions (Mn^{2+}, Ni^{2+}, Co^{2+}). Noteworthy is that complexes $Mn(hfac)_2L^{Et}$,

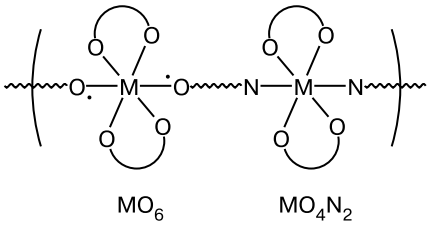

Fig. 13. Alternation scheme of the MO_6 and MO_4N_2 coordination units in the "head-to-head"-type chains.

Table 4. Changes in the $M—O_L$ and $M—N_L$ bond lengths (d) in solid solutions $Mn_xCu_{1-x}(hfac)_2L^{Et}$ and $Co_xCu_{1-x}(hfac)_2L^{Et}$ at different ratios Mn : Cu or Co : Cu (T = 295 K)

Mn : Cu			Co : Cu		
ratio	d/Å		ratio	d/Å	
	$M—O_L$	$M—N_L$		$M—O_L$	$M—N_L$
1 : 0	2.156	2.299	1 : 0	2.071	2.180
0.46 : 0.54	2.171	2.375			
0.22 : 0.78	2.185	2.375	0.19 : 0.81	2.236	2.284
0.15 : 0.85	2.224	2.375	0.08 : 0.92	2.237	2.350
0 : 1	2.237	2.375	0 : 1	2.237	2.375

$Co(hfac)_2L^{Et}$, and $Ni(hfac)_2L^{Et}$ exhibit no anomalies in the $\mu_{eff}(T)$ plots. As an example we present the temperature dependence of μ_{eff} for $Mn(hfac)_2L^{Et}$ (Fig. 14), which points to strong antiferromagnetic exchange interaction in the exchange clusters >N—˙O—Mn^{2+}—O˙—N<; because of this, the μ_{eff} value tends to the theoretical limit (5 μ_B) on cooling.

We also carried out a single-crystal X-ray diffraction study of $Mn(hfac)_2L^{Et}$ at different temperatures and found that structural rearrangement of the coordination units of $Mn(hfac)_2L^{Et}$ on cooling are fundamentally different from those of $Cu(hfac)_2L^{Et}$. If the distances $Cu—O_L$ in the CuO_6 unit of $Cu(hfac)_2L^{Et}$ increase in the order 2.237 Å (293 K) → 2.260 Å (188 K) → 2.281 Å (115 K), the initially shorter distances $Mn—O_L$ in $Mn(hfac)_2L^{Et}$ are gradually shortened as follows: 2.156 Å (295 K) → 2.143 Å (200 K) → 2.140 Å (115 K), thus providing a typical examples of compression of solids on cooling. The distances $Mn—N_L$ in the coordination units MnO_4N_2 are also lengthened only slightly (2.299 (295 K) → 2.281 (200 K) → 2.276 Å (115 K)). For comparison, changes in the $Cu—N_L$ distances in $Cu(hfac)_2L^{Et}$ are much more pronounced (2.375 (293 K) → 2.079 (188 K) → → 2.055 Å (115 K)).

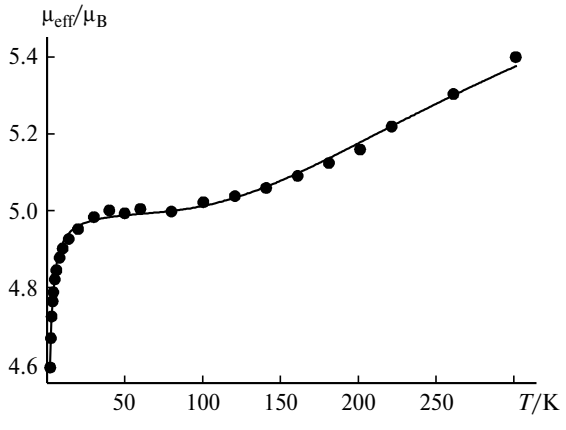

Fig. 14. Temperature dependence of μ_{eff} for $Mn(hfac)_2L^{Et}$ (full circles denote experimental data and the solid curve represents the results of calculations).

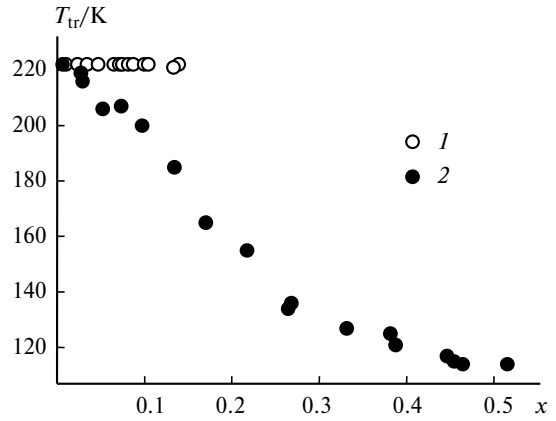

Fig. 15. Phase transition temperatures of solid solutions $Ni_xCu_{1-x}(hfac)_2L^{Et}$ (*1*) and $Mn_xCu_{1-x}(hfac)_2L^{Et}$ (*2*) plotted *vs*. their compositions.

Replacement of copper atoms by Mn and Ni (or Co) atoms in different coordination units affects the magnetic properties of corresponding solid solutions in different manner. For instance, the transition temperature of solid solutions $Mn_xCu_{1-x}(hfac)_2L^{Et}$ monotonically decreases from 220 to 115 K as x increases from 0 to ~0.5. At $x > 0.5$, the transition is completely suppressed by manganese (Fig. 15). Substitution in the system $Ni_xCu_{1-x}(hfac)_2L^{Et}$ causes no pronounced changes in the transition temperature until $x \approx 0.2$ (see Fig. 15); the transition is suppressed in the range $0.15 < x < 0.25$.

The experimental dependences $\mu_{eff}(T)$ obtained for mixed-metal solid solutions at different x show that an increase in x in the system $Mn_xCu_{1-x}(hfac)_2L^{Et}$ causes a decrease in the transition temperature and makes the transition more "diffuse" (Fig. 16, *a*). In other words, introduction of Mn ions makes the MO_6 units and the whole crystal more "rigid". Therefore, the crystal must be cooled to a lower temperature for the phase transition to occur in order to attain structural rearrangement of the remaining coordination units CuO_6 containing the exchange clusters >N—•O—Cu^{2+}—O•—N<. This was experimentally confirmed by the results of a single-crystal X-ray diffraction study of $Mn_{0.22}Cu_{0.78}(hfac)_2L^{Et}$ solid solution at different temperatures. It was found that the distances M—O_L in the MO_6 polyhedra change with temperature in the order 2.185 (295 K) → 2.162 (220 K) → 2.152 (180 K) → → 2.140 (140 K) → 2.159 Å (110 K) and the distances Cu—N_L in the CuO_4N_2 polyhedra change as follows: 2.375 (295 K) → 2.326 (220 K) → 2.308 (180 K) → 2.289 (140 K) → 2.315 Å (110 K). Comparison of these changes with those of the corresponding to distances in $Mn(hfac)_2L^{Et}$ and $Cu(hfac)_2L^{Et}$ (see above) shows that manganese does significantly suppress the dynamics of the MO_6 coordination units (at $x = 0.22$, Mn atoms occupy nearly 50% of these units). In this case, the crystal must be cooled to much lower temperatures in order to

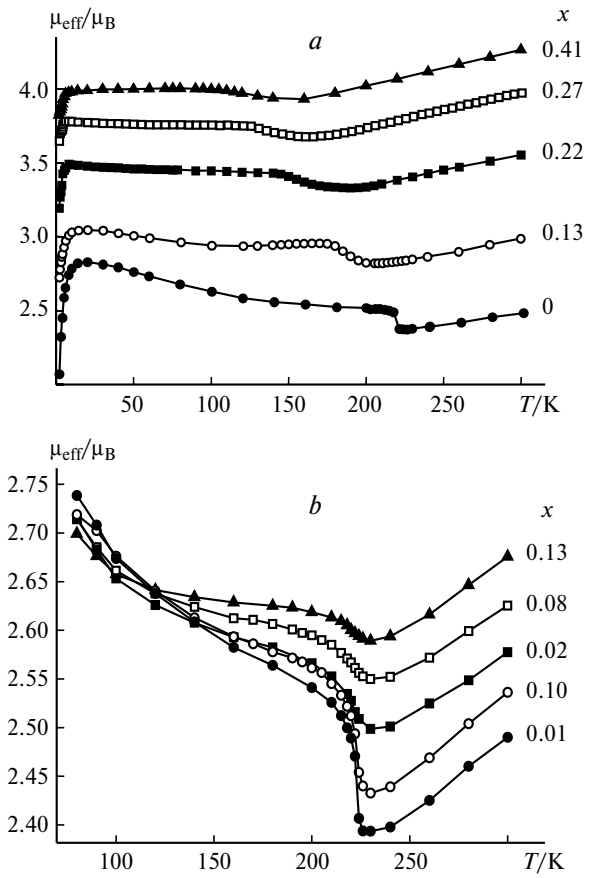

Fig. 16. Dependences $\mu_{eff}(T,x)$ for $Mn_xCu_{1-x}(hfac)_2L^{Et}$ (*a*) and $Ni_xCu_{1-x}(hfac)_2L^{Et}$ (*b*).

attain structural rearrangement of the remaining coordination units CuO_6 containing the exchange clusters >N—•O—Cu^{2+}—O•—N< in which the exchange interaction changes its sign. These data show that the jumpwise lengthening of the averaged distance M—O_L in $Mn_{0.22}Cu_{0.78}(hfac)_2L^{Et}$ occurs only on cooling below 140 K, which is in excellent agreement with the results of magnetochemical experiment (see Fig. 16). Hampering changes in the MO_6 units, manganese atoms thus also preclude changes in the CuO_4N_2 units. If at room temperature the Cu—N_L distances in $Mn_{0.22}Cu_{0.78}(hfac)_2L^{Et}$ are the same as those in $Cu(hfac)_2L^{Et}$ (2.375 Å), on cooling of $Mn_{0.22}Cu_{0.78}(hfac)_2L^{Et}$ they are shortened much slower and much smaller than in $Cu(hfac)_2L^{Et}$. At $x = 0.5$, Mn^{2+} ions occupy all the MO_6, units and there are no longer CuO_6 units whose structural rearrangement is responsible for the magnetic anomaly.

At small x ($x \approx 0.15$), solid solutions $Ni_xCu_{1-x}(hfac)_2L^{Et}$ and $Co_xCu_{1-x}(hfac)_2L^{Et}$ retain their transition temperatures (see Fig. 15) and then ($x > 0.2$) the phase transition is abruptly suppressed. This can be explained as follows. First, in contrast to Mn ions, Ni (or Co) ions are present in the MO_4N_2 but not CuO_6 units

whose dynamics is responsible for the onset of the magnetic effect. Second, Ni^{2+} and Co^{2+} have nearly the same ionic radii as Cu^{2+}. Therefore, introduction of small amounts of Ni^{2+} and Co^{2+} ions ($x \le 0.15$) into the MO_4N_2 units causes no significant structure distortion of $Cu(hfac)_2L^{Et}$; as a consequence, the temperature of the magnetic feature is retained (see Figs. 15 and 16, *b*). However, after reaching some critical values x (>0.2) the non-Jahn—Teller ions, Ni^{2+} or Co^{2+}, introduced into the MO_4N_2 units significantly change their dynamics and thus indirectly preclude changes in the coordination units CuO_6. This seems to be quite reasonable, because lengthening of the Cu—O distances in the exchange clusters >N—˙O—Cu^{2+}—O˙—N< is accompanied by considerable shortening of the distances Cu—N_L in the CuO_4N_2 units (see above). Since at $x > 0.2$ analogous changes in the NiO_4N_2 (or CoO_4N_2) units seem to be impossible, the total number of the CuO_6 units capable of producing the magnetic effect also rapidly decreases. However, below the critical values of x the structural dynamics of the CuO_6 and MO_4N_2 units in the transition region retain their character. For instance, below the transition point the trend of changes in the M—O_L and M—N_L bond lengths of $Ni_{0.08}Cu_{0.92}(hfac)_2L^{Et}$ is the same as that observed for $Cu(hfac)_2L^{Et}$. On cooling the distances d(M—O_L) increase jumpwise at ~220 K as follows: (2.222 (240 K) → 2.223 (220 K) → 2.245 Å (200 K)), whereas the distances M—N_L are shortened (2.245 (240 K) → 2.148 (220 K) → 2.104 Å (200 K)).

Occurrence of Mn^{2+} (Ni^{2+}) ions in the MO_6 (MO_4N_2) units at $x < 0.5$ (see Fig. 13) was also confirmed in a study of the magnetic properties of solid solutions. The data presented below show that the experimental dependences $\mu_{eff}(T)$ cannot be described using the *reductio ad absurdum* hypothesis. The optimum parameters of the spin Hamiltonian for the description of the magnetic properties of $Cu(hfac)_2L^{Et}$ (separately for the regions above and below the phase transition), $Mn(hfac)_2L^{Et}$, and $Ni(hfac)_2L^{Et}$ are presented in Table 5. The calculated values are in good agreement with the experimental dependences $\mu_{eff}(T)$ (see Fig. 14, the theoretical curve was calculated using the parameters listed in Table 5). The experimental dependences $\mu_{eff}(T)$ for the solid solutions $Mn_{0.57}Cu_{0.43}(hfac)_2L^{Et}$ (Table 6 and Fig. 17) and $Ni_{0.44}Cu_{0.56}(hfac)_2L^{Et}$ (see Table 6), in which Mn or Ni occupy nearly 50% of the coordination units, can be approximated assuming two opposite types of arrangement of the metal ions, namely, the metal atoms replaces Cu atoms in the CuO_6 units or in the CuO_4N_2 units. The results obtained for two versions of theoretical approximation are listed in Table 6.

Table 5. Optimum parameters of the spin-Hamiltonian* for the description of the magnetic properties of complexes $M(hfac)_2L^{Et}$

Compound	g_M	J/K	$J'z$/K
$Cu(hfac)_2L^{Et}$ ($T < 220$ K)	2.0	41.7	−0.6
$Cu(hfac)_2L^{Et}$ ($T > 230$ K)	2.52	−121	−0.34
$Mn(hfac)_2L^{Et}$	2.0	−110	−0.017
$Ni(hfac)_2L^{Et}$	2.33	−368	−1.0

* $\hat{H} = -2J(\hat{s}_{NO}\hat{s}_M + \hat{s}_M\hat{s}_{NO}) - \beta(2g_M\hat{s}_M + 2g_{NO}\hat{s}_{NO})H - 2J'z\hat{S}\langle\hat{S}\rangle$; the spin-Hamiltonian includes the spin—spin interaction in the exchange cluster, Zeeman interaction, and weak chain—chain and cluster—cluster interactions.[25]

Table 6. Parameters of the temperature dependences of μ_{eff} for $Mn_{0.57}Cu_{0.43}(hfac)_2L^{Et}$ and $Ni_{0.44}Cu_{0.56}(hfac)_2L^{Et}$ calculated assuming that Mn or Ni atoms replace Cu atoms in the MO_6 (*1*) and MO_4N_2 units (*2*)

No.	$Mn_{0.57}Cu_{0.43}(hfac)_2L^{Et}$				$Ni_{0.44}Cu_{0.56}(hfac)_2L^{Et}$			
	g_{Mn}	g_{Cu}	J/K	$J'z$/K	g_{Ni}	g_{Cu}	J/K	$J'z$/K
1	2.09	2.56	−111	−0.14	1.36	3.92	−234	−2.9
2	1.50	3.18	−200	−0.06	2.06	1.92	−138	−0.84

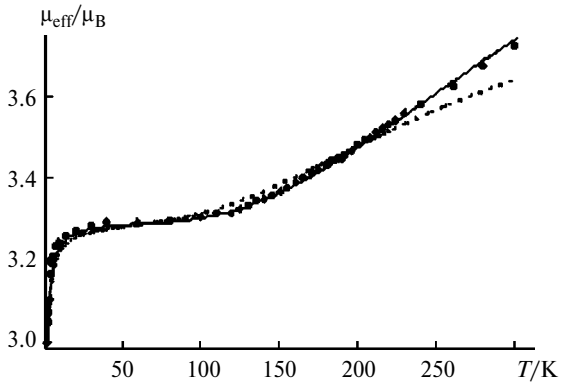

Fig. 17. Temperature dependence of μ_{eff} for $Mn_{0.57}Cu_{0.43}(hfac)_2L^{Et}$ (full circles denote experimental data and the solid curves represent the results obtained for different versions of optimization).

The experimental dependences $\mu_{eff}(T)$ are correctly described using the parameters listed in lines *1* ($Mn_{0.57}Cu_{0.43}(hfac)_2L^{Et}$) and *2* ($Ni_{0,44}Cu_{0,56}(hfac)_2L^{Et}$). *Vice versa*, line *2* for $Mn_{0.57}Cu_{0.43}(hfac)_2L^{Et}$ and line *1* for $Ni_{0,44}Cu_{0,56}(hfac)_2L^{Et}$ contain non-realistic g_M and g_{Cu} values. A more illustrative example is provided by the plots of two versions of theoretical approximation of the experimental data for $Mn_{0.57}Cu_{0.43}(hfac)_2L^{Et}$ shown in Fig. 17. The solid curve calculated using the parameters listed in line *1* of Table 6 correctly describes the experimental values $\mu_{eff}(T)$, whereas the dashed curve calculated using the parameters listed in line *2* of Table 6 deviates from the experimental data in the high-temperature region.

Thus, the results of studies on the structure and magnetic properties of solid solutions $M_xCu_{1-x}(hfac)_2L^{Et}$ sug-

gest that at $x \leq 0.5$ Mn atoms replace Cu atoms in the coordination units CuO_6 while Ni (or Co) atoms replace Cu atoms in the coordination units CuO_4N_2. This is a very important result because it offers the possibility of controllable modification of the character of the $\mu_{eff}(T)$ dependence in the spin transition region.

Solid solutions $Cu(hfac)_2L^{Me}{}_xL^{Et}{}_{1-x}$

The possibility of formation of solid solutions $Cu(hfac)_2L^{Me}{}_xL^{Et}{}_{1-x}$ was quite attractive because compounds $Cu(hfac)_2L^{Me}$ and $Cu(hfac)_2L^{Et}$ are characterized by basically different temperature dependences of μ_{eff} (see Figs. 1 and 9). Moreover, the $Cu(hfac)_2L^{Me}$ and $Cu(hfac)_2L^{Et}$ polymorphs exhibiting magnetic features also have different structural motifs of polymer chains, namely, "head-to-tail" for the former and "head-to-head" for the latter compound (see Figs. 2 and 8, respectively). We succeeded to obtain solid solutions $Cu(hfac)_2L^{Me}{}_xL^{Et}{}_{1-x}$[29] in spite of significant differences between the chain structure and the volume occupied by the paramagnetic ligand molecules L^{Me} and L^{Et}. The formation of solid solutions $Cu(hfac)_2L^{Me}{}_xL^{Et}{}_{1-x}$ is undoubtedly an advance because solid solutions of complexes containing different organic ligands are rare in occurrence compared to solid solutions of mixed-metal complexes.[1]

What type of changes in the magnetic effect (*i.e.*, in character of the temperature dependence of μ_{eff}) with increasing x in the solid solutions $Cu(hfac)_2L^{Me}{}_xL^{Et}{}_{1-x}$ could be expected from general considerations? We could assume that ligand L^{Me}, whose molecules are smaller than the L^{Et} molecules, can gradually (at least until $x \approx 0.5$) replace the L^{Et} molecules by embedding into the dominating "head-to-head"-type chains of $Cu(hfac)_2L^{Et}$ taking into account that some $Cu(hfac)_2L^{Me}$ polymorphs also have this chain motif (see above). As a result, at small x the character of the magnetic anomaly in the $\mu_{eff}(T)$ plots for $Cu(hfac)_2L^{Me}{}_xL^{Et}{}_{1-x}$ must be the same as that observed for $Cu(hfac)_2L^{Et}$. The temperature of the magnetic anomaly would be shifted because replacement of L^{Et} by L^{Me} is inequivalent. In the vicinity of $x \approx 0.5$ the situation becomes uncertain because L^{Et} and L^{Me} are now present in comparable amounts. In this case, the structural type of the solid phase formed (namely, a "head-to-head" $Cu(hfac)_2L^{Et}$-like or a "head-to-tail" $Cu(hfac)_2L^{Me}$-like structure, a mixture of phases, or a new phase) is to a great extent determined by kinetic factors because individual compounds $Cu(hfac)_2L^{Et}$ and $Cu(hfac)_2L^{Me}$ have similar solubilities. It is much easier to make assumptions about the region $x > 0.6$. Here, the content of L^{Me} is higher and it is quite logical to assume that the solid solution formed must have a "head-to-tail" rather than "head-to-head" structural motif and, hence, the shape of the magnetic feature in the $\mu_{eff}(T)$ plot for $Cu(hfac)_2L^{Me}{}_xL^{Et}{}_{1-x}$ must become similar to that typical of $Cu(hfac)_2L^{Me}$. The closer the x value to unity, the more the temperature of the magnetic anomaly must be closer to 146 K (characteristic value for $Cu(hfac)_2L^{Me}$).

Indeed, it is these changes in the shape of the magnetic anomaly for $Cu(hfac)_2L^{Me}{}_xL^{Et}{}_{1-x}$ that were observed experimentally (Fig. 18, *a*). At $0 < x < \sim 0.5$, the character of the temperature dependence of μ_{eff} for $Cu(hfac)_2L^{Me}{}_xL^{Et}{}_{1-x}$ remains the same as for $Cu(hfac)_2L^{Et}$. An increase in the L^{Me} content increasingly suppresses the transition and its realization requires a deeper cooling of $Cu(hfac)_2L^{Me}{}_xL^{Et}{}_{1-x}$. In the region $x \approx 0.5$—0.6 the magnetic anomaly practically disappears and at $x > 0.6$ it reappears, being at the same time typical of $Cu(hfac)_2L^{Me}$. It is of great importance that the $\mu_{eff}(T)$ curves correspond to individual compounds $Cu(hfac)_2L^{Me}{}_xL^{Et}{}_{1-x}$ and exhibit no impurity features of the phases $Cu(hfac)_2L^{Et}$ or $Cu(hfac)_2L^{Me}$.

A severe problem in estimation of x in the studies of $Cu(hfac)_2L^{Me}{}_xL^{Et}{}_{1-x}$ solutions with different organic ligands is to determine the content of L^{Me} and L^{Et}. In this Section the as symbols "x" and "$1 - x$" denote only the L^{Et} : L^{Me} ratio in the starting reaction mixture. Compounds $Cu(hfac)_2L^{Et}$ and $Cu(hfac)_2L^{Me}$ have similar solubilities (see above). Taking into account the fact that at synthesis of solid solutions, they were nearly quantitatively isolated from the mother liquor, we can assume that the mole ratio L^{Et} : L^{Me} in the solid phases is similar to that in the starting reagent mixture. However, it is desired to elaborate an analytical technique suitable for measuring the amounts of simultaneously present ligands L^{Me} and L^{Et}.

In this case the use of IR spectroscopy and a specially synthesised isotopically substituted product containing a CD_3 group instead of CH_3 group in the pyrazole ring (hereafter, this ligand is denoted as L^{CD_3}) appeared to be efficient.[29] General trends in the character of changes in the $\mu_{eff}(T)$ dependences for $Cu(hfac)_2L^{Me}{}_xL^{Et}{}_{1-x}$ and $Cu(hfac)_2L^{CD_3}{}_xL^{Et}{}_{1-x}$ are retained (see Fig. 18, *b*). However, a very important remark should be made. The results obtained for one of the two complexes, $Cu(hfac)_2L^{Me}{}_xL^{Et}{}_{1-x}$ or $Cu(hfac)_2L^{CD_3}{}_xL^{Et}{}_{1-x}$, should not be transferred to the other complex. This appeared to be quite unexpected because our study of products containing L^{CD_3} revealed a specific manifestation of the isotope effect, which deserves particular consideration. Now we will discuss the isotope effect and then return to the solid solutions $Cu(hfac)_2L^{CD_3}{}_xL^{Et}{}_{1-x}$.

Isotope effect

Prior to determining the x value for solid solutions, single crystals of paramagnetic ligand L^{CD_3} were grown and the ligand structure was investigated. The molecular

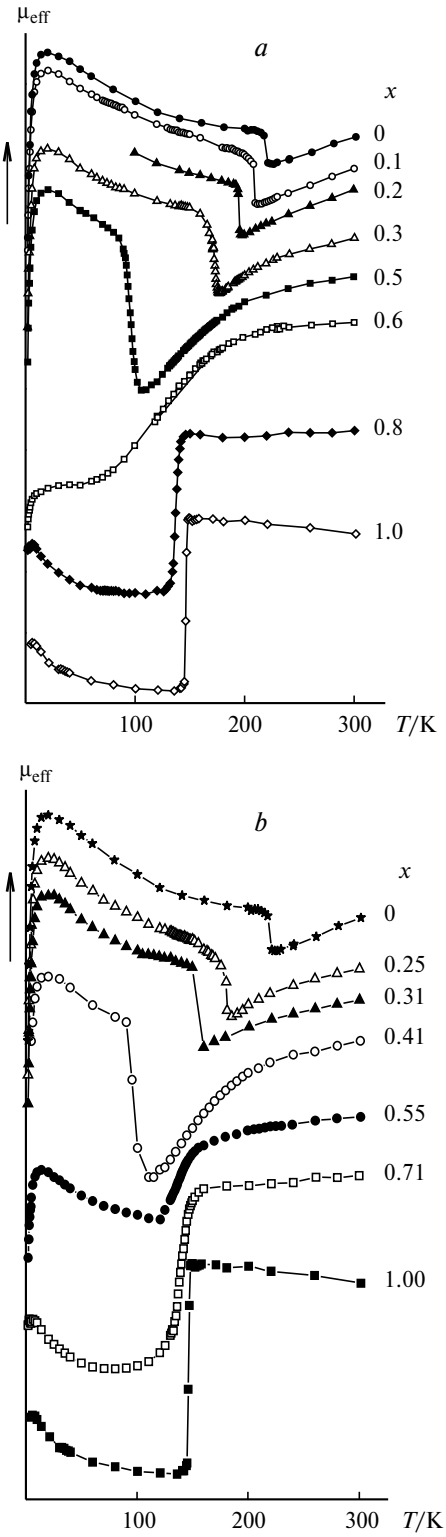

Fig. 18. Experimental temperature dependences of μ_{eff} for $Cu(hfac)_2L^{Me}{}_xL^{Et}{}_{1-x}$ (*a*) and $Cu(hfac)_2L^{CD_3}{}_xL^{Et}{}_{1-x}$ (*b*) (for clarity, the curves are shifted along the ordinate axis).

structures of L^{CD_3} and L^{Me} were found to be identical within the limits of experimental errors. For instance, the N—O bond lengths are equal to 1.280±0.003 Å for both L^{Me} and L^{CD_3}. The angle between the plane formed by the atoms of pyrazole ring and the plane passing through the atoms of CN_2 group of the O˙—N—C=N→O fragment of imidazolyl ring is 3.7±0.3° for both L^{Me} and L^{CD_3}. To confirm structural similarity of $Cu(hfac)_2L^{Me}$ and $Cu(hfac)_2L^{CD_3}$, crystals of different $Cu(hfac)_2L^{CD_3}$ polymorphs were grown and investigated.[30] Their magnetic properties were compared with the properties of the corresponding $Cu(hfac)_2L^{Me}$ polymorphs and it was found that changes in structural parameters of the "head-to-head" polymeric chain polymorphs of $Cu(hfac)_2L^{Me}$ and $Cu(hfac)_2L^{CD_3}$ obey the same pattern. Therefore, it is not surprising that both complexes (with deuterated and nondeuterated ligands) exhibit nearly identical magnetic properties.

Naturally, similar correlations between the magnetic properties and structure of compounds should also be expected for the $Cu(hfac)_2L^{Me}$ and $Cu(hfac)_2L^{CD_3}$ polymorphs with "head-to-tail" packed polymer chains. Therefore, it was quite surprising that both the chemical and magnetic properties of the complex with L^{CD_3} appeared to be different from the properties of the complex with L^{Me}.

We established that the reaction of $Cu(hfac)_2$ with L^{CD_3} carried out under the synthesis conditions of the "head-to-tail-1" phase of $Cu(hfac)_2L^{Me}$ resulted in nearly equiprobable formation of "head-to-tail-1" or "head-to-tail-2" $Cu(hfac)_2L^{CD_3}$ crystals or in their mixture, which was separated mechanically. Usually, the major component of the mixture was the "head-to-tail-2" polymorph. This was not observed in the reaction of $Cu(hfac)_2L$ with L^{Me}. The "head-to-tail-1" phase of $Cu(hfac)_2L^{Me}$ was isolated with ease from solutions of a 1 : 1 mixture of $Cu(hfac)_2$ and L^{Me} in hexane and heptane or in mixtures with more polar solvents (hexane—acetone, hexane—Et_2O). Isolation of the "head-to-tail-2" polymorph of $Cu(hfac)_2L^{Me}$ was a complicated task. This phase was obtained at a 3 : 2 ratio of the starting reagents, $Cu(hfac)_2$ and L^{Me}, which were dissolved in a heptane—CH_2Cl_2 (~10 : 1) mixture on heating; then, the mother liquor was filtered quickly. A few minutes later, two types of freshly formed dark blue crystals with slightly different habits were immediately filtered. The most part of crystals were the "head-to-tail-1" $Cu(hfac)_2L^{Me}$ crystals mixed with the "head-to-tail-2" $Cu(hfac)_2L^{Me}$ crystals that can be mechanically separated. However, the amount of the "head-to-tail-2" polymorph obtained using this version of the synthetic procedure is always very small (if exists). It is important that the first portion of crystals should be filtered quickly a short time (5 to 15 min) after mixing of reagents and cooling of the solution. If the reaction mixture is stored for a long time, the solid phase contains only $[Cu(hfac)_2]_3L^{Me}{}_2 \cdot C_7H_{16}$. And only owing to the fact that the crystals of $[Cu(hfac)_2]_3L^{Me}{}_2 \cdot C_7H_{16}$ are formed rather slowly, it is possible to isolate and then separate a mixture

Table 7. Temperature dependences of the structural parameters of $Cu(hfac)_2L^{CD_3}$ and $Cu(hfac)_2L^{Me}$

Chain packing motif	Space group	T/K	Cu—O_L	Cu—N_L	Angle CN_2—Pz
			d/Å		α/deg
		$Cu(hfac)_2L^{CD_3}$			
"head-to-tail-1"	$P2_1/n$	295	2.477(3)	2.308(3)	5.4(6)
"head-to-tail-2"	$P\bar{1}$	155	2.478(3)	2.307(4)	6.3(6)
			2.480(3)	2.308(4)	10.0(7)
		120	1.958(11)	1.970(14)	2(2)
			2.391(11)	2.268(13)	13.2(2.5)
		$Cu(hfac)_2L^{Me}$			
"head-to-tail-1"	$P2_1/n$	295	2.484(5)	2.329(5)	13.3(6)
"head-to-tail-2"	$P\bar{1}$	140	1.992(9)	2.014(10)	1.4(1.5)
			2.449(9)	2.336(10)	11.3(1.7)

of the "head-to-tail-1" and "head-to-tail-2" polymorphs which quickly precipitates out of the mother liquor.[28]

Considering the structures of the "head-to-tail-1" and "head-to-tail-2" polymorphs of $Cu(hfac)_2L^{CD_3}$ and comparing them with, *e.g.*, the structure of the "head-to-tail-1" polymorph of $Cu(hfac)_2L^{Me}$, we can say that the complexes with L^{CD_3} are structurally different from the complex with L^{Me} (though this was not *a priori* expected). Some parameters of the "head-to-tail-1" and "head-to-tail-2" polymorphs of $Cu(hfac)_2L^{CD_3}$ differ appreciably, being also strongly different from those of $Cu(hfac)_2L^{Me}$ (see Table 7). The main difference between the structural characteristics is the magnitude of the angle between the plane formed by the atoms of pyrazole ring and the plane passing through the CN_2 atoms of the O$^{\bullet}$—N—C=N→O fragment of imidazole ring. At present, we cannot explain why replacement of CH_3 group by CD_3 group caused this angle to be nearly halved (!). However, this structural change affects the magnetic properties. The $\mu_{eff}(T)$ plots obtained for both $Cu(hfac)_2L^{CD3}$ polymorphs exhibit a shift of the transition region toward higher temperatures (Fig. 19). Indeed, the transition temperatures of the "head-to-tail-1" and "head-to-tail-2" phases of $Cu(hfac)_2L^{Me}$ are 146(↓) and 148(↑) K, whereas those of the "head-to-tail-1" and "head-to-tail-2" polymorphs of $Cu(hfac)_2L^{CD_3}$ are 149(↓) and 151(↑) K. In other words, deuteration of methyl substituent in the pyrazole ring of the paramagnetic ligand led to particular changes in structure of the solid phase of $Cu(hfac)_2L^{CD_3}$ and, as a consequence, to a 3 K increase in the transition temperature of this complex compared to $Cu(hfac)_2L^{Me}$. The magnitude of this effect is of course small; however, the effect does occur and can be reproducibly detected.

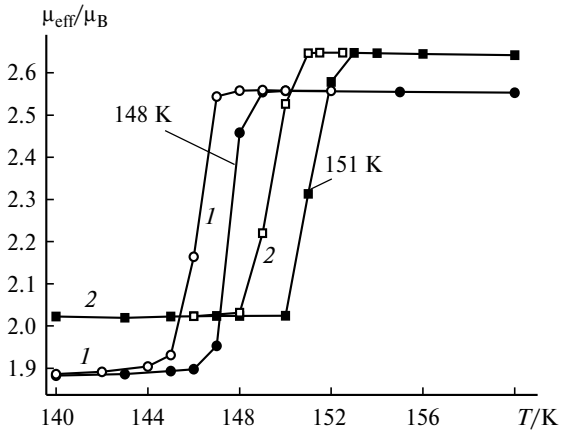

Fig. 19. Temperature dependences of μ_{eff} for $Cu(hfac)_2L^{Me}$ (*1*) and $Cu(hfac)_2L^{CD_3}$ (*2*).

Noteworthy is also a similar character of the $\mu_{eff}(T)$ dependences obtained for the "head-to-tail-1" $Cu(hfac)_2L^{CD_3}$ and "head-to-tail-2" $Cu(hfac)_2L^{CD_3}$ polymorphs. The structures of these phases are slightly different, but in this case even minor structural changes can strongly affect the magnetic properties of compounds.[28] A structural dynamics study of the "head-to-tail-1" polymorph of $Cu(hfac)_2L^{CD_3}$ revealed an irreversible transformation into the "head-to-tail-2" phase on cooling similarly to the case of the "head-to-tail-1" polymorph of $Cu(hfac)_2L^{Me}$, which clarifies the reason for identical shape of the temperature dependences of μ_{eff}. However, the difference between the polymorphous transformation temperatures of $Cu(hfac)_2L^{Me}$ (230±1 K) and $Cu(hfac)_2L^{CD_3}$ (235±1 K) is again reproducibly detected. It should also be noted that the crystals of $Cu(hfac)_2L^{CD_3}$ are more "elastic", *i.e.*, they are more stable on going through the transition region.

Thus, we have to note that correlations between the magnetic properties and structure of $Cu(hfac)_2L^{CD_3}{}_xL^{Et}{}_{1-x}$, should not be automatically transferred to solid solutions $Cu(hfac)_2L^{Me}{}_xL^{Et}{}_{1-x}$. Experimental data obtained for $Cu(hfac)_2L^{CD_3}{}_xL^{Et}{}_{1-x}$ can include a small isotope effect. The contribution of this effect can hardly be assessed because the deuterium label was introduced exclusively for analytical determination of the x value and we had no independent method for the same purpose. Otherwise, we could correctly compare correla-

tions between the magnetic properties and structure of $Cu(hfac)_2L^{CD_3}{}_xL^{Et}{}_{1-x}$ and $Cu(hfac)_2L^{Me}{}_xL^{Et}{}_{1-x}$ at the same x and distinguish the contribution of the isotope effect (if any).

Solid solutions $Cu(hfac)_2L^{CD_3}{}_xL^{Et}{}_{1-x}$

Crystals of solid solutions $Cu(hfac)_2L^{CD_3}{}_xL^{Et}{}_{1-x}$ appeared to be mechanically stable over a wide temperature range. This allowed us to study the structural dynamics at different temperatures and to reveal some features accompanying the phase transition. The $\mu_{eff}(T)$ plot obtained for $Cu(hfac)_2L^{CD_3}{}_{0.31}L^{Et}{}_{0.69}$ (the x value was determined with an accuracy of ± 0.03) is shown in Fig. 18, *b*. Changes in the Cu—O_L and Cu—N_L distances are most pronounced; the corresponding data are listed in Table 8. The structure of $Cu(hfac)_2L^{CD_3}{}_{0.31}L^{Et}{}_{0.69}$ was investigated above (at 240 K) and below (120 K) the magnetic anomaly, and at the transition temperature (155 K). The midpoint of this temperature interval characterizes the transition region between the high-temperature and low-temperature phases, so our study at 155 K permitted assessment of the actual structure of the transition state. It was found that before transition to the low-temperature phase the Cu—O_L distances in the CuO_6 units of the exchange clusters >N—$^{\bullet}$O—Cu^{2+}—O$^{\bullet}$—N< are appreciably shortened and then abruptly increase. *Vice versa*, the Cu—N_L distances in the CuN_2O_4 units are lengthened prior to being abruptly shortened.

The crystal structure of $Cu(hfac)_2L^{CD_3}{}_{0.41}L^{Et}{}_{0.59}$ solid solution characterized by a magnetic anomaly temperature of 100 K (see Fig. 18, *b*) was established at 240, 170, and 110 K (see Table 8), *i.e.*, in the high-temperature phase. The results obtained are in excellent agreement with those reported for $Cu(hfac)_2L^{CD_3}{}_{0.31}L^{Et}{}_{0.69}$ and clearly demonstrate a stage of pre-compression of CuO_6 units and pre-expansion of CuN_2O_4 units.

The $Cu(hfac)_2L^{CD_3}{}_{0.31}L^{Et}{}_{0.69}$ and $Cu(hfac)_2L^{CD_3}{}_{0.41}L^{Et}{}_{0.59}$ crystals are comprised of "head-to-head" packed chains typical of $Cu(hfac)_2L^{Et}$ (see Fig. 8). As mentioned above, at $x > 0.6$ the "head-to-tail" motif typical of $Cu(hfac)_2L^{Me}$ dominates and the crystal system is changed from monoclinic to triclinic. Our study of $Cu(hfac)_2L^{CD_3}{}_{0.71}L^{Et}{}_{0.29}$ showed that the character of the $\mu_{eff}(T)$ dependence (see Fig. 18, *b*) is similar to that of $Cu(hfac)_2L^{Me}$ (see Fig. 1). On going to the low-temperature phase the Cu—O_L and Cu—N_L distances in 50% of CuO_5N units are appreciably shortened (Table 9), which is responsible for spin pairing in 50% of exchange clusters Cu^{2+}—O$^{\bullet}$—N< and, as a consequence, for the decrease in μ_{eff} by a factor of $\sqrt{2}$. A structural study of $Cu(hfac)_2L^{CD_3}{}_{0.71}L^{Et}{}_{0.29}$ crystals in the transition region is a very complicated task because of crystal cracking. By and large, single crystals of solid solutions with $x < 0.4$ ($Cu(hfac)_2L^{Et}$ packing motif) are mechanically more stable than single crystals of solutions with $x > 0.6$ ($Cu(hfac)_2L^{Me}$ packing motif). The reasons for this phenomenon are unclear. As mentioned above, cooling or heating of this type of crystals is accompanied by intense co-operative dynamic processes. Since these processes occur "far" from the exchange clusters Cu^{2+}—O$^{\bullet}$—N<, which are of prime importance for understanding the magnetic anomaly, we will not dwell on them. However, a very important difference between the chain packing motifs in the structures of $Cu(hfac)_2L^{Et}$ and $Cu(hfac)_2L^{Me}$ deserves attention. In the "head-to-tail" $Cu(hfac)_2L^{Me}$ crystals, all chains are aligned. But in $Cu(hfac)_2L^{Et}$ and all other $Cu(hfac)_2L^{R}$ crystals with the "head-to-head" packing motif chains are aligned only within alternating parallel layers in which chains in one layer make an angle with chains in another layer (Fig. 20). It cannot be ruled out that the possibility of layer slip in crystals with the "head-to-head" chain packing motif makes them more elastic.

Studies in the transition region ($0.4 < x < 0.6$) characterized by a change in the polymer chain motifs in solid solutions $Cu(hfac)_2L^{CD_3}{}_xL^{Et}{}_{1-x}$ faced severe problems. The reason is that formation of a certain phase depends on many uncontrollable kinetic parameters. Here, construction of the phase diagram (as in the case of solid solutions of transition metal complexes with nitroxyl radicals[31—34]) was impossible because the reaction mixtures stored over 1—2 days contained not only the growing crystals of $Cu(hfac)_2L^{CD_3}{}_xL^{Et}{}_{1-x}$ (or $Cu(hfac)_2L^{Me}{}_xL^{Et}{}_{1-x}$) but also decomposition products.

Table 8. Temperature dependences of the structural parameters of solid solutions $Cu(hfac)_2L^{CD_3}{}_{0.31}L^{Et}{}_{0.69}$ and $Cu(hfac)_2L^{CD_3}{}_{0.41}L^{Et}{}_{0.59}$

T/K	d(Cu—O_L)/Å	d(Cu—N_L)/Å
	$Cu(hfac)_2L^{CD_3}{}_{0.31}L^{Et}{}_{0.69}$	
240	2.241(4)	2.337(4)
155	2.131(1)	2.351(4)
120	2.293(3)	2.070(4)
	$Cu(hfac)_2L^{CD_3}{}_{0.41}L^{Et}{}_{0.59}$	
240	2.264(2)	2.338(3)
170	2.183(3)	2.353(3)
110	2.062(3)	2.367(3)

Table 9. Temperature dependences of the structural parameters of solid solutions $Cu(hfac)_2L^{CD_3}{}_{0.71}L^{Et}{}_{0.29}$

T/K	d(M—O_L)/Å	d(M—N_L)/Å	CN_2—Pz angle/deg
240	2.425(3)	2.293(4)	6.5(6)
	2.478(3)	2.321(4)	7.4(7)
110	1.982(4)	2.019(4)	1.5(7)
	2.419(4)	2.322(5)	10.9(8)

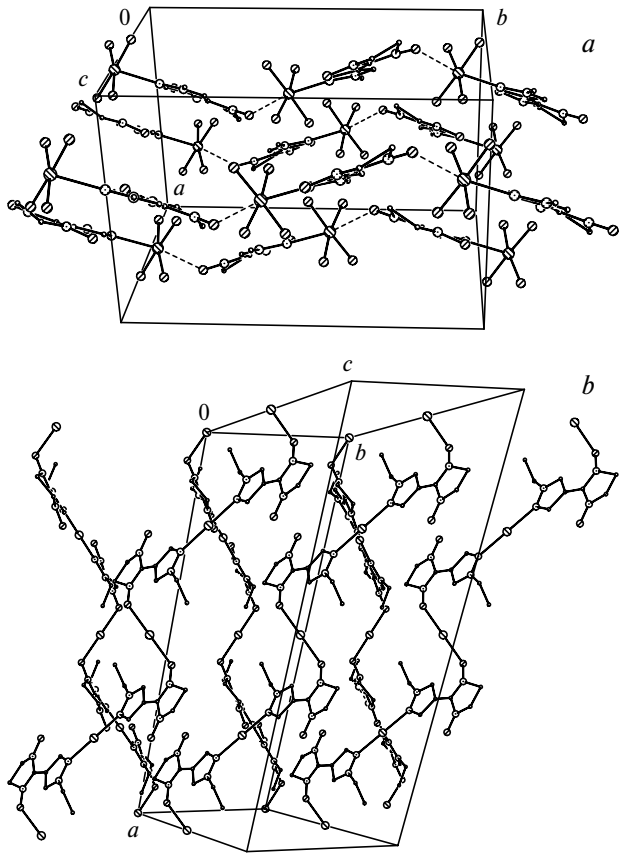

Fig. 20. Chain packing in the structures of $Cu(hfac)_2L^{Me}$ (*a*) and $Cu(hfac)_2L^{Et}$ (*b*).

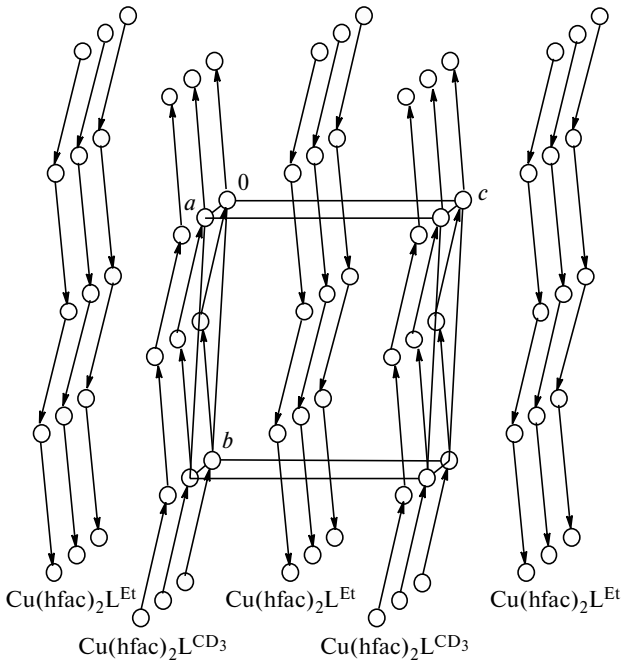

Fig. 21. $Cu(hfac)_2L^{CD_3}$ and $Cu(hfac)_2L^{Et}$ chain packing to form layers in the solid phase of $Cu(hfac)_2L^{CD_3}{}_{0.55}L^{Et}{}_{0.45}$. Copper atoms are denoted by open circles (hfac anions are not shown). Arrows denote oppositely directed bridging ligands L^R within the layers comprised of the $Cu(hfac)_2L^{CD_3}$ and $Cu(hfac)_2L^{Et}$ chains.

In fact, all solid solutions discussed in this work were obtained in the kinetic regime rather than under thermodynamic equilibrium conditions because the complexes are unstable in solution and can form a variety of polymorphs (see above). Nevertheless, multiple repetition of experiments with solid solutions with $x < 0.4$ and $x > 0.6$ under similar conditions gave well reproducible results. This suggests that they are formed under quasi-equilibrium conditions. At $0.4 < x < 0.6$, the crystals formed were, as a rule, nonhomogeneous and the dependences $\mu_{eff}(T)$ for the solid phases obtained in different experiments were often different.

The aforesaid incessantly stimulated our interest in the $Cu(hfac)_2L^{CD_3}{}_{0.5}L^{Et}{}_{0.5}$ phase called a "50 : 50" phase. We failed to grow crystals of this phase. However, is became insignificant after we grew and structurally characterized single crystals $Cu(hfac)_2L^{CD_3}{}_{0.55}L^{Et}{}_{0.45}$ with similar composition. Of particular interest is that the paramagnetic ligands L^{CD_3} and L^{Et} are not randomly distributed within the crystal, as could be assumed. The structure of the solid phase of $Cu(hfac)_2L^{CD_3}{}_{0.55}L^{Et}{}_{0.45}$ can be considered as being comprised of alternating polymer layers formed by the "head-to-tail" $\{Cu(hfac)_2L^{CD_3}\}_\infty$ chains or $\{Cu(hfac)_2L^{Et}\}_\infty$ chains. The bridging ligands L^R inside one type of layers are "directed" in one direction, whereas in the other type of layers they are "directed" in another direction (Fig. 21), *i.e.*, each polymer chain contains only one type of organic radicals. Because the whole crystal is an ordered system with long-range order rather than aggregate of chains and layers, $Cu(hfac)_2L^{CD_3}{}_{0.5}L^{Et}{}_{0.5}$ is an individual chemical compound. Would construction of the equilibrium phase diagram be possible, the diagram should separate into at least two regions, namely, the region of solid solutions $[Cu(hfac)_2L^{Et}—Cu(hfac)_2L^{CD_3}{}_{0.5}L^{Et}{}_{0.5}]$ and the region of solid solutions $[Cu(hfac)_2L^{CD_3}{}_{0.5}L^{Et}{}_{0.5}—Cu(hfac)_2L^{CD_3}]$.

Consider the structure and structural dynamics of $Cu(hfac)_2L^{CD_3}{}_{0.55}L^{Et}{}_{0.45}$ on temperature variation in more detail. The chains $\{Cu(hfac)_2L^{CD_3}\}_\infty$ "force" the $\{Cu(hfac)_2L^{Et}\}_\infty$ chains to adopt an atypical "head-to-tail" motif. Here, one crystallographically independent chain contains only the ligand L^{CD_3} while the other crystallographically independent chain contains only the ligand L^{Et}. In this chain, carbon atoms of the methyl fragment of ethyl group are located with a statistical weight of nearly unity. This is quite natural because the content of L^{Et} in the system under study is somewhat less than 50%. The $Cu—O_L$ and $Cu—N_L$ bond lengths and the angles α between the plane formed by atoms of the pyrazole ring and the plane passing through the CN_2 atoms of the $O^{\bullet}—N—C=N→O$ fragment of imidazole ring for the

Table 10. Temperature dependences of structural parameters of the system $Cu(hfac)_2L^{CD_3}{}_{0.55}L^{Et}{}_{0.45}$

Parameter	Ligand	240 K		150 K		110 K	
		Cu(1)	Cu(2)	Cu(1)	Cu(2)	Cu(1)	Cu(2)
Bond				*d*/Å			
$Cu—O_L$	L^{CD_3}	2.410(7)	2.492(9)	2.310(5)	2.463(6)	2.033(6)	2.432(9)
	L^{Et}	2.434(7)	2.489(8)	2.324(6)	2.446(6)	2.046(7)	2.412(8)
$Cu—N_L$	L^{CD_3}	2.361(9)	2.354(9)	2.251(7)	2.364(7)	2.048(8)	2.303(11)
	L^{Et}	2.274(8)	2.322(9)	2.229(6)	2.279(7)	2.043(10)	2.321(11)
Angle				α/deg			
$CN_2—Pz$	L^{CD_3}	8.4(1.9)	11.6(6)	8.5(1.3)	10.2(4)	3.3(1.4)	9.2(8)
	L^{Et}	6.5(1.3)	6.9(1.6)	5.4(1.0)	8.9(1.2)	0.5(1.0)	8.7(1.6)

chains in $\{Cu(hfac)_2L^{CD_3}\}_\infty$ and $\{Cu(hfac)_2L^{Et}\}_\infty$ are listed in Table 10. As temperature decreases, the bond lengths $Cu—O_L$ and $Cu—N_L$ are gradually and then abruptly (on going through the magnetic anomaly region; T_c = 138 K, see Fig. 18, *b*) shortened. This occurs only in 50% of CuO_5N units. In the other 50% of CuO_5N units these bond lengths are only slightly shortened. Besides, if before the transition the angles α were similar in magnitude, after the transition they become significantly different. These changes are similar to those described for solid solution $Cu(hfac)_2L^{CD_3}{}_{0.71}L^{Et}{}_{0.29}$ (see Table 9) or "head-to-tail-2" polymorph of $Cu(hfac)_2L^{CD_3}$ (see Table 7).

Conclusion

The results presented in this review show that investigations of stereochemically nonrigid systems based on $Cu(hfac)_2$ and nitroxyl radicals, in which spin transitions can occur, is a non-trivial problem complicated by the possibility of existence of various of polymorphs whose magnetic properties are strongly influenced by minor structure variations. At the same time the variety of structural motifs predetermines the diversity of magnetic effects. Of particular interest is also the fact that the solid phases of all compounds exhibiting the magnetic anomalies have a polymeric rather than simple molecule-based structure. This requires a very high degree of co-operation in motion of polymer chains relative to one another on going from one polymorph to another without destruction of the crystal.

Heterospin systems based on copper(II) complexes with nitroxyl radicals are of particular interest for detailed studies of various structural phase transitions that induce magnetic anomalies similar to spin crossover. Despite the small number of compounds exhibiting these effects, the magnetic transitions were observed in a wide temperature range (30—250 K). The upper bound of transition temperatures is only limited by the decomposition temperatures of complexes and can be estimated at 350—400 K. A valuable feature of the heterospin complexes under study is that they can be obtained as high-quality single crystals that are mechanically stable over a wide temperature range. Studies on correlations between the structural dynamics and character of changes in the magnetic properties can provide unique information for subsequent quantum-chemical analysis of the electronic structure of exchange clusters. Besides, these complexes contain readily functionalizable paramagnetic ligands, which offers prospects for better insight into the structural dynamics of the whole compound in the phase transition region, elucidation of factors responsible for the character of the $\mu_{eff}(T)$ dependence, and development of methods for controllable modification of characteristics of the magnetic transition *via* pre-design of paramagnetic ligands with a desired structure. It is of great importance that the temperature and character of these effects can also be controlled by preparing mixed-metal solid solutions and solid solutions of complexes with different paramagnetic ligands.

This work was financially supported by the U.S. Civilian Research & Development Foundation (CRDF Grant NO-008-X1, Y1-C-08-03), Russian Foundation for Basic Research (Project Nos. 03-03-32518, 02-03-33112, and 04-03-08002), Russian Federation Ministry of Education and Science (Grant E02-5.0-188), Presidium of the Russian Academy of Sciences, Chemistry and Materials Science Branch of the of the Russian Academy of Sciences, and the Siberian Branch of the Russian Academy of Sciences.

References

1. P. Gütlich, A. Hauser, and H. Spiering, *Angew. Chem., Int. Ed. Engl.*, 1994, **33**, 2024.
2. O. Kahn, *Molecular Magnetism*, VCH, New York, 1993.
3. M. Bacci, *Coord. Chem. Rev.*, 1988, **86**, 245.
4. H. A. Goodwin, *Coord. Chem. Rev.*, 1976, **18**, 293.
5. O. Kahn, J. Krober, and C. Jay, *Adv. Mater.*, 1992, **4**, 718.
6. E. Konig, G. Ritter, and S. K. Kulshreshthsa, *Chem. Rev.*, 1985, **85**, 219.
7. E. Konig, *Progr. Inorg. Chem.*, 1987, **35**, 527.

8. E. Konig, *Structure and Bonding*, 1991, **76**, 51.
9. H. Toftlund, *Chem. Rev.*, 1989, **94**, 67.
10. V. V. Zelentsov, *Koord. Khim.*, 1992, **18**, 787 [*Russ. J. Coord. Chem.*, 1992, **18** (Engl. Transl.)].
11. V. V. Zelentsov, *Ross. Khim. Zh.*, 1996, **40**, 86 [*Mendeleev Chem. J.*, 1996, **40** (Engl. Transl.)].
12. L. G. Lavrenova and S. V. Larionov, *Koord. Khim.*, 1998, **24**, 403 [*Russ. J. Coord. Chem.*, 1998, **24**, 379 (Engl. Transl.)].
13. F. Lanfranc de Panthou, E. Belorizky, R. Calemczuk, D. Luneau, C. Marcenat, E. Ressouche, P. Turek, and P. Rey, *J. Am. Chem. Soc.*, 1995, **117**, 11247.
14. F. Lanfranc de Panthou, D. Luneau, R. Musin, L. Öhrström, A. Grand, P. Turek, and P. Rey, *Inorg. Chem.*, 1996, **35**, 3484.
15. P. Rey and V. I. Ovcharenko, in *Magnetism: Molecules to Materials IV*, Eds J. S. Miller and M. Drillon, Wiley-VCH, 2003, 41.
16. F. Iwahory, K. Inoue, and H. Iwamura, *Mol. Cryst. Liq. Cryst.*, 1999, **334**, 533.
17. A. Caneschi, P. Chiesi, L. David, F. Ferraro, D. Gatteschi, and R. Sessoli, *Inorg. Chem.*, 1993, **32**, 1445.
18. V. I. Ovcharenko, S. V. Fokin, G. V. Romanenko, Yu. G. Shvedenkov, V. N. Ikorskii, E. V. Tretyakov, and S. F. Vasilevskii, *Zh. Strukt. Khim.*, 2002, **43**, 163 [*Russ. J. Struct. Chem.*, 2002, **43**, 153 (Engl. Transl.)].
19. V. I. Ovcharenko, S. V. Fokin, G. V. Romanenko, V. N. Ikorskii, E. V. Tretyakov, S. F. Vasilevsky, and R. Z. Sagdeev, *Mol. Phys.*, 2002, **100**, 1107.
20. V. I. Ovcharenko, S. V. Fokin, G. V. Romanenko, Yu. Shvedenkov, V. N. Ikorskii, E. V. Tretyakov, and S. F. Vasilevsky, *Abstr. 3d Intern. Conf. on Nitroxide Radicals (Kaizerslautern, Germany, Sept., 2001)*, Kaizerslautern (Germany), 2001, 28.
21. V. Ovcharenko, S. Fokin, G. Romanenko, Y. Shvedenkov, V. Ikorskii, E. Tretyakov, and S. Vasilevsky, *Abstr. XXXV Intern. Conf. on Coordination Chemistry (Heidelberg, Germany, July, 2002)*, Heidelberg (Germany), 2002, 151.
22. Yu. A. Osip´yan, R. B. Morgunov, A. A. Baskakov, V. I. Ovcharenko, and S. V. Fokin, *Fizika Tverdogo Tela*, 2003, **45**, 1396 [*Sov. Phys. Sol. State*, 2003, **45**, 1465 (Engl. Transl.)].
23. R. N. Musin, P. V. Schastnev, and S. A. Malinovskaya, *Inorg. Chem.*, 1992, **31**, 4118.
24. R. N. Musin, I. V. Ovcharenko, L. Öhrström, and P. Rey, *Zh. Strukt. Khim.*, 1997, **38**, 840 [*Russ. J. Struct. Chem.*, 1997, **38**, 703 (Engl. Transl.)].
25. R. N. Musin, I. V. Ovcharenko, L. Öhrström, and P. Rey, *Zh. Strukt. Khim.*, 1997, **38**, 850 [*Russ. J. Struct. Chem.*, 1997, **38**, 711 (Engl. Transl.)].
26. I. V. Ovcharenko, Yu. G. Shvedenkov, R. N. Musin, and V. N. Ikorskii, *Zh. Strukt. Khim.*, 1999, **40**, 36 [*Russ. J. Struct. Chem.*, 1999, **40**, 29 (Engl. Transl.)].
27. V. I. Ovcharenko, *Abstr. VII Int. Conf. on Molecule-Based Magnets (San Antonio, Texas, USA, September 16—21, 2000)*, San Antonio (Texas, USA), 2000, 48.
28. S. Fokin, V. Ovcharenko, G. Romanenko, and V. Ikorskii, *Inorg. Chem.*, 2004, **43**, 969.
29. K. Yu. Maryunina, S. V. Fokin, E. V. Tretyakov, G. V. Romanenko, V. N. Ikorskii, R. Z. Sagdeev, and V. I. Ovcharenko, *Tez. dokl. II Vseros. konf. "Vysokospinovye molekuly i molekulyarnye magnetiki" [Abstr. 2nd All-Russia Conf. on High-Spin Molecules and Molecule-Based Magnetics] (Novosibirsk, Russia, May 14—17, 2004)*, Novosibirsk, 2004, 54 (in Russian).
30. G. V. Romanenko, K. Yu. Maryunina, V. N. Ikorskii, V. I. Ovcharenko, and R. Z. Sagdeev, *Tez. dokl. II Vseros. konf. "Vysokospinovye molekuly i molekulyarnye magnetiki" [Abstr. 2nd All-Russia Conf. on High-Spin Molecules and Molecule-Based Magnetics] (Novosibirsk, Russia, May 14—17, 2004)*, Novosibirsk, 2004, 104 (in Russian)
31. E. Yu. Fursova, V. N. Ikorskii, G. V. Romanenko, V. A. Reznikov, Yu. G. Shvedenkov, and V. I. Ovcharenko, *Zh. Strukt. Khim.*, 2002, **43**, 706 [*Russ. J. Struct. Chem.*, 2002, **43**, 656 (Engl. Transl.)].
32. E. Fursova, Y. Shvedenkov, G. Romanenko, V. Ikorskii, and V. Ovcharenko, *Abstr. VII Intern. Conf. on Molecule-Based Magnets (San Antonio, Texas, USA, September 16—21, 2000)*, San Antonio (Texas, USA), 2000, 230.
33. E. Yu. Fursova, G. V. Romanenko, Yu. G. Shvedenkov, V. N. Ikorskii, V. A. Reznikov, and V. I. Ovcharenko, *Abstr. XXth Chugaev Int. Conf. on Coord. Chemistry (Rostov-on-Don, Russia, June 25—29, 2001)*, 2001, 462.
34. E. Yu. Fursova, V. N. Ikorskii, G. V. Romanenko, V. A. Reznikov, Yu. G. Shvedenkov, and V. I. Ovcharenko, *Tez. dokl. I Vseros. konf. "Vysokospinovye molekuly i molekulyarnye ferromagnetiki" [Abstr. 1st All-Russia Conf. on High-Spin Molecules and Molecule-Based Ferromagnetics] (Chernogolovka, Russia, March 18—21, 2002)*, 2002, 19 (in Russian).

Received May 28, 2004